Figure 1

a.

b.

Figure 1: Typical findings of the two types of HCC in the hepatobiliary phase of gadoxetic acid–enhanced axial MR imaging. **(a)** On image obtained in the hepatobiliary phase (20 minutes after injection of gadoxetic acid) in a 62-year-old woman, a hypointense HCC shows definitely lower SI. **(b)** In contrast, image of iso- or hyperintense HCC obtained in 66-year-old man shows almost higher SI, with a portion showing lower SI relative to the surrounding enhanced liver.

Two pathologists (Y.Z. and Y.N. [with 37 years of experience]) diagnosed each nodule according to the classification proposed by the International Working Party (26) and the World Health Organization classification (27): well, moderately, or poorly differentiated HCC. Then, HCCs were classified into four proliferative patterns—namely, trabecular, pseudoglandular, solid, and scirrhous patterns. We compared hypointense HCCs and iso- or hyperintense HCCs with regard to histologic features such as tumor differentiation, proliferation pattern, and the presence of bile plugs.

Polymerase Chain Reaction Analysis

The expression of OATP-A, OATP-B, OATP-C, OATP8, MRP1, MRP2 and MRP3 messenger RNA was examined by means of reverse transcription polymerase chain reaction (PCR) in HCCs and the surrounding liver tissue in 22 livers (Table 2) from which we could obtain fresh-frozen specimens. In the remaining 18 livers, the frozen specimens were not preserved. β-Actin was used as an internal reference. Primer sequences and product sizes are shown in Table E1 (online).

Next, we quantitatively examined messenger RNA expression levels of seven transporters in the same 22 livers by using real-time PCR. Specific primers and probes for seven transporters and β-actin were obtained from Applied Biosystems (Warrington, England). For quantitative evaluation of the expression of each transporter, we used the tumor/background expression score, defined as (tumor transporter value/tumor β-actin value)/(background transporter value/background β-actin value). Then, we examined the correlation of the transporter expression score and the enhancement ratio in the hepatobiliary phase of gadoxetic acid–enhanced MR imaging.

Immunohistochemical Analysis

According to the results of reverse transcription PCR, which indicated that OATP8 would be the key uptake transporter, immunostaining of OATP8 was performed for all HCCs by using a primary antibody against human OATP8 (mouse monoclonal, NB100–74482; Novus Biologicals, Littleton, Colo) (1:100). After removal of the specimen from the paraffin, antigen retrieval was performed by microwaving it in an edetic acid buffer (pH, 8.0) for 20 minutes. Two abdominal imaging radiologists (A.K. and N.Y. [with 7 years of experience]) semiquantitatively evaluated the intensity of OATP8 expression on the tumor cellular membrane in comparison with that of nonneoplastic hepatocytes as follows: A grade of 0 indicated no expression; a grade of 1+, decreased expression; a grade of 2+, equivalent expression; and a grade of 3+, increased expression. We used the grade at the largest area of each nodule.

Dual immunofluorescence staining of OATP8 and coagulation factor VIII, a marker of endothelial cells, was performed to examine whether or not OATP8 is expressed on the sinusoidal side of carcinoma cells. We used the previously described antibody for human OATP8 and rabbit polyclonal antibody for human factor VIII (A0082; Dako Cytomation, Glostrup, Denmark).

The details of the experiments (reverse transcription PCR and immunostaining) were as described in the article by Nakamura et al (28).

Overall Assessment

A schematic for the molecular background of the dynamics of gadoxetic acid in HCC cells as considered from our study was developed.

Statistical Analysis

Statistical significance was evaluated with software (Prism5; GraphPad Software, San Diego, Calif). The unpaired *t* test was used for the analysis of clinical features and quantitative reverse transcription PCR results, the Fisher exact test and the χ^2 test were used for the analysis of clinical and histologic features, the Friedman test was used for the time-SI curve, the Mann-Whitney test was used for the immunohistochemical findings, and the Pearson correlation test was used for the correlations between quantitative reverse transcription PCR and the enhancement ratio. $P < .05$ was considered to indicate a statistically significant difference.

Results

Clinical Features of the Two Types of HCCs

Thirty-two nodules were classified as hypointense HCCs, and eight nodules

Figure 2

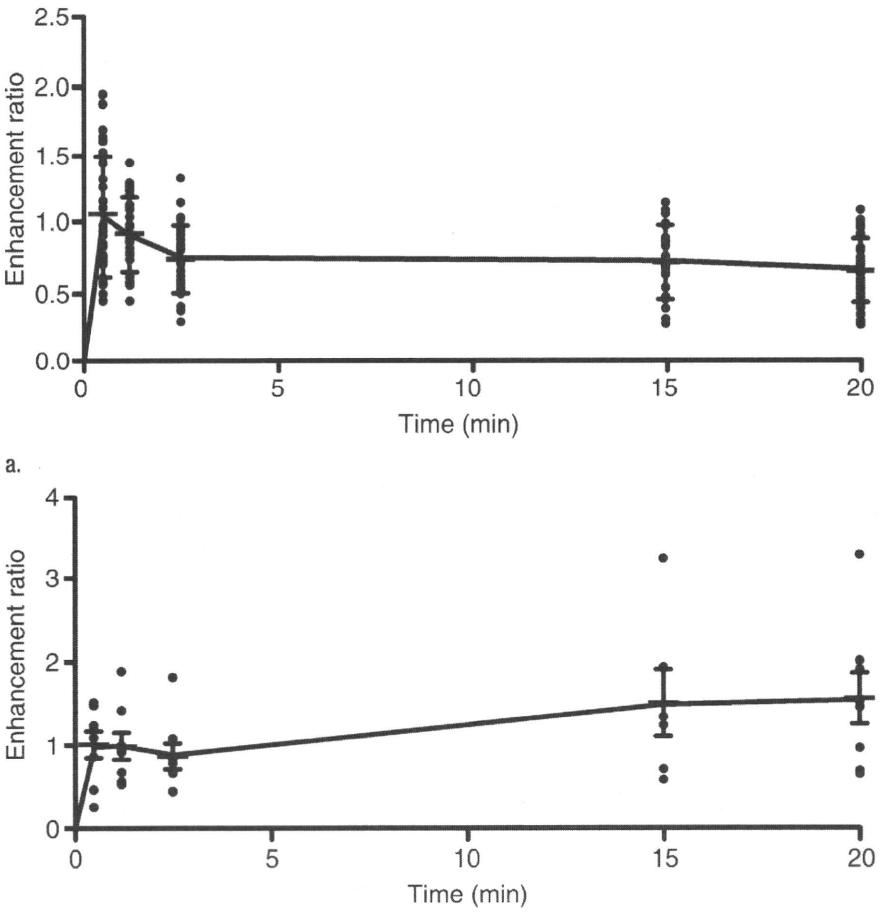

Figure 2: Time-SI curves at gadoxetic acid–enhanced MR imaging. Both hypointense HCCs and iso- or hyperintense HCCs show a rapid, increasing pattern in the arterial or the portal phase. **(a)** In hypointense HCCs, enhancement ratio decreases from the equilibrium phase to the hepatobiliary phase. **(b)** In contrast, iso- or hyperintense HCCs show increasing curves from the equilibrium phase to the hepatobiliary phase. $P < .001$. Enhancement ratio = (pre-enhancement SI minus postenhancement SI)/pre-enhancement SI.

were classified as iso- or hyperintense HCCs. No significant differences in any clinical features were observed between the two types (Table 1).

Time-SI Curves at Gadoxetic Acid–enhanced MR Imaging

Both the hypointense HCCs and the iso- or hyperintense HCCs showed a spike-like rapid increase of enhancement ratio in the arterial phase. After the equilibrium phase, the enhancement ratio decreased in hypointense HCCs; in contrast, iso- or hyperintense HCCs showed increasing intensity curves ($P < .001$) (Fig 2).

Messenger RNA Expression of Hepatocyte Membrane Transporters

OATP8 was constantly expressed in the background nonneoplastic portions of the livers. However, its expression was slight in all hypointense HCCs. In contrast, OATP8 expression was evident in all iso- or hyperintense HCCs (Fig 3). According to the results of real-time quantitative reverse transcription PCR (Fig 4; Fig E2 [online]), the degree of OATP8 expression in all hypointense HCCs was less than that in background livers (tumor/background expression score, <1.0), and was higher in iso- or hyperintense HCCs than in background livers (tumor/background expression score, >1.0) ($P < .001$).

The expression of MRP3, an export transporter on the sinusoidal side, was also lower in hypointense HCCs and was preserved in iso- or hyperintense HCCs, with a significant difference ($P < .001$). No significant difference was observed in the expression levels of the other transporters between the two types of HCCs ($P = .07$–$.53$). MRP2, a major export transporter on the canalicular side, was constantly expressed in all HCCs (Figs 3, 4; Fig E2 [online]).

There was a significant correlation between the tumor/background expression score of OATP8 and enhancement ratio in the hepatobiliary phase of gadoxetic acid–enhanced MR imaging ($P < .001$, $R = 0.84$) (Fig 5).

Immunohistochemistry of OATP8

In the nonneoplastic liver, OATP8 was expressed on the cellular membrane of hepatocytes at the sinusoidal side. In iso- or hyperintense HCCs, OATP8 was similarly expressed on the cellular membrane of HCC cells. In contrast, the degree of OATP8 expression in hypointense HCCs was clearly weaker than that in nonneoplastic liver ($P < .001$) (Figs 6, 7).

At double immunostaining of OATP8 and coagulation factor VIII in iso- or hyperintense HCCs, OATP8 was expressed on the sinusoidal side labeled by factor VIII in iso- or hyperintense HCCs (Fig E3 [online]). That is, in iso- or hyperintense HCCs, OATP8 expression was sustained on the cellular membrane at the sinusoidal side—the same as in nonneoplastic hepatocytes.

Pathologic Features of the Two Types of HCCs

Seven (88%) of eight iso- or hyperintense HCCs were moderately differentiated, and six (75%) of eight showed a predominantly pseudoglandular pattern, while seven (88%) of eight were associated with bile production (bile plugs). On the other hand, the hypointense HCCs consisted of three cases of well-differentiated, 25 cases of moderately differentiated, and four cases of poorly differentiated HCCs; the trabecular proliferation pattern was most

Table 2

Clinical, Histologic, and Radiologic Features in 22 Patients in Whom PCR Data Were Available

Patient Sex/Age (y)	Tumor Size (cm)	Differentiation	Proliferation Pattern	Bile Plugs	Gadoxetic Acid–enhanced MR Imaging Appearance
M/58	3.5	Moderate	Trabecular	Absent	Hypointense
M/77	14.5	Moderate	Pseudoglandular	Present	Hypointense
M/65	2.6	Moderate	Pseudoglandular	Present	Hypointense
M/78	8.8	Moderate	Solid	Absent	Hypointense
F/71	3.0	Moderate	Trabecular	Absent	Hypointense
M/60	2.5	Well	Pseudoglandular	Present	Hypointense
F/63	1.3	Well	Trabecular	Absent	Hypointense
F/60	1.8	Moderate	Trabecular	Absent	Hypointense
M/68	2.0	Well	Trabecular	Absent	Hypointense
M/63	3.8	Moderate	Trabecular	Absent	Hypointense
F/61	9.5	Moderate	Trabecular	Absent	Hypointense
M/60	5.2	Poor	Trabecular	Absent	Hypointense
M/52	7.2	Moderate	Trabecular	Absent	Hypointense
F/75	3.5	Moderate	Trabecular	Absent	Hypointense
F/63	3.3	Moderate	Pseudoglandular	Present	Hypointense
M/61	3.7	Moderate	Trabecular	Absent	Hypointense
M/57	2.0	Moderate	Trabecular	Absent	Hypointense
M/65	2.4	Moderate	Pseudoglandular	Present	Hyperintense
F/52	10.5	Moderate	Pseudoglandular	Present	Hyperintense
M/74	2.5	Well	Trabecular	Absent	Hyperintense
M/66	2.8	Moderate	Pseudoglandular	Present	Hyperintense
M/76	6.0	Moderate	Pseudoglandular	Present	Hyperintense

Figure 3

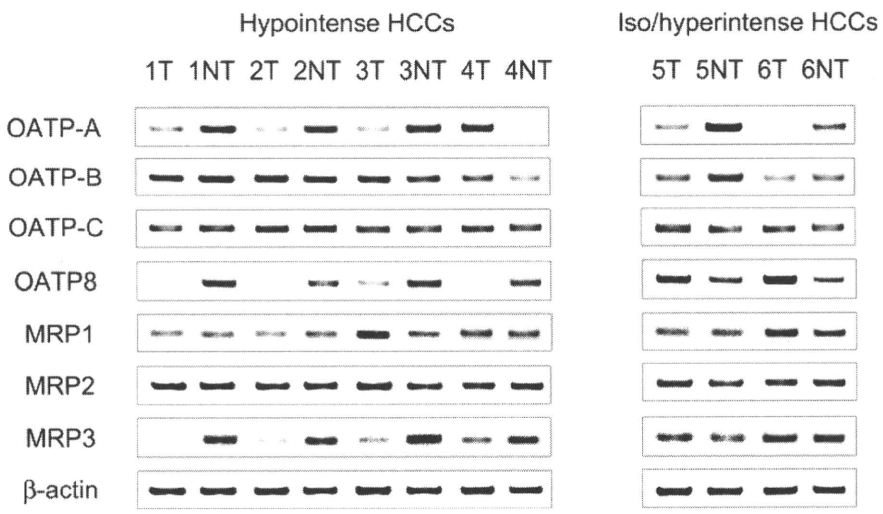

Figure 3: Results of reverse transcription PCR for hepatocellular transporters. Data in six typical cases of HCC are shown; the remaining cases also showed similar results. All transporters are almost constantly expressed in the background nonneoplastic livers. Expression of OATP8, an uptake transporter, is weak in hypointense HCCs (cases 1–4). In contrast, its expression in iso- or hyperintense HCCs is higher than that in background liver (cases 5–6). Expression of MRP3, an export transporter on the sinusoidal side, is also lower in hypointense HCCs and is preserved in iso- or hyperintense HCCs. There are no clear differences in the expression levels of the other five transporters (OATP-A, OATP-B, OATP-C, MRP1, and MRP2) between the two groups. *NT* = nontumor, *T* = tumor.

common (23 [72%] of 32 cases), whereas the pseudoglandular pattern and bile production were also observed in some cases (six [19%] and 10 [31%] cases, respectively). There was no significant difference compared with the occurrence in hypointense HCCs ($P = .57$). In contrast, there were significant differences in proliferation patterns and bile production between the two types of HCCs ($P = .01$ and $P = .006$, respectively) (Fig 8).

Figure 9 shows the molecular background of the dynamics of gadoxetic acid in HCC cells in our study. In iso- or hyperintense HCCs, a large amount of gadoxetic acid would be taken up from the tumor blood sinusoids into HCC cells by OATP8 and be gradually excreted again into tumor blood sinusoids by not MRP2 but MRP3, probably because of the depletion of bile ducts in the HCCs. On the other hand, the uptake of gadoxetic acid might be blocked or reduced because of the lower expression of OATP8 in hypointense HCCs.

Discussion

It has been reported that, uniquely among hepatic malignant tumors, some HCCs show iso- or hyperintensity in the hepatobiliary phase of gadoxetic acid–enhanced MR imaging (4,7). It has been suggested that this is reflective of the degree of residual hepatobiliary function or grade of tumor differentiation (11,12); however, to our knowledge, no basic studies are available to support these contentions. To clarify the mechanism underlying this finding, we performed an imaging-molecular-pathologic correlation study to compare HCCs that were hypointense to surrounding liver with those that were iso- or hyperintense.

Time-SI curves in hypointense HCCs showed a decrease in the SI of the tumor after the dynamic phase that continued to the hepatobiliary phase. This decreasing pattern corresponds to the so-called washout of contrast material from the tumor blood spaces commonly seen in hypervascular HCCs in the equilibrium phase of dynamic MR imaging with gadopentetate dimeglumine (10).

Figure 4

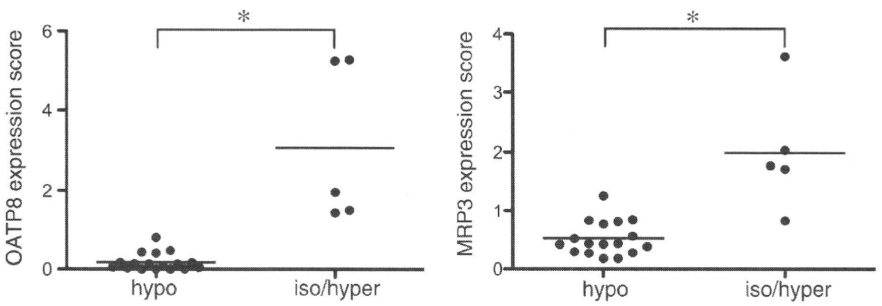

Figure 4: Graphs show results of quantitative real-time PCR of transporters. Hypointense HCCs *(hypo)* have significantly lower expression levels of **(a)** OATP8 and **(b)** MRP3 messenger RNA compared with iso- or hyperintense HCCs *(iso/hyper)* (* = $P < .001$). Expression score = (tumor transporter value/tumor β-actin value)/(background transporter value/background β-actin value). Tumor enhancement ratio = (pre-enhancement SI minus postenhancement SI)/pre-enhancement SI (in hepatobiliary phase).

Figure 5

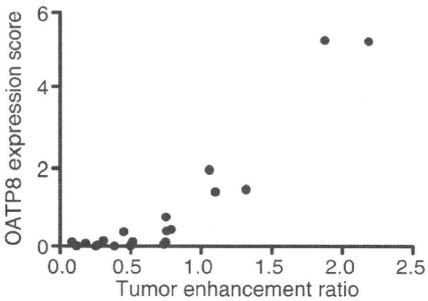

Figure 5: Correlation of OATP8 expression at PCR and tumor enhancement ratio in the hepatobiliary phase. There is a significant correlation between the tumor/background expression score of OATP8 and enhancement ratio in the hepatobiliary phase of gadoxetic acid–enhanced MR imaging. $P < .001$, $R = 0.84$. Expression score = (tumor transporter value/tumor β-actin value)/(background transporter value/background β-actin value). Enhancement ratio = (pre-enhancement SI minus postenhancement SI)/pre-enhancement SI.

This suggests that the decreasing pattern of the curve reflects the decline of the contrast medium in the tumor blood spaces and that the tumor cells hardly take up gadoxetic acid. In contrast, iso- or hyperintense HCCs demonstrated an increasing curve. This indicates that the uptake of gadoxetic acid is greater than the washout in iso- or hyperintense HCCs.

The PCR and immunostaining results showed that the OATP8 expression level was significantly higher in the iso- or hyperintense HCCs and significantly lower in hypointense HCCs than in the surrounding liver. In addition, the OATP8 expression level in HCCs was significantly and positively correlated with the enhancement ratio in the hepatobiliary phase of gadoxetic acid–enhanced MR imaging. Immunostaining also verified the location of OATP8 on the sinusoidal-side membrane of iso- or hyperintense HCC cells—the same as in nonneoplastic hepatocytes. On the basis of these results, we conclude that OATP8 is the best candidate among the four OATPs we tested to help determine the uptake of gadoxetic acid in HCC cells.

An important point is that particularly OATP8 is involved in the uptake of gadoxetic acid in HCC cells. Narita et al (29) recently reported similar results to ours. They also verified that there was a significant correlation between the enhancement ratio in the hepatobiliary phase and the expression level of OATP1B3 (synonymous with OATP8 [20]) protein at Western blot analysis in HCCs. However, their study focused solely on OATP1B3 and did not analyze the involvement of any other transporters. Therefore, the mechanisms of transporters in gadoxetic acid uptake were not elucidated in their entirety. We examined other possible transporters, because transporters can compensate to some extent for the functions of others, especially in disrupted conditions. Indeed, OATP8 and OATP-C share 80% of their amino acid sequences, and can transport some common substrates into cells (17). In our study, we showed that OATP8 and MRP3 expression correlated with enhancement ratio in HCCs, whereas the other five transporters containing OATP-C showed no significant correlations. However, it may be that the expression level does not always correspond with the functional level of a transporter. To examine the functional levels of OATP8 and the other transporters, further studies using cultures of purified hepatocytes from hypointense and iso- or hyperintense HCCs are needed.

MRP3 is an export transporter of organic anions on the sinusoidal side of hepatocytes. Its expression was significantly increased in iso- or hyperintense HCCs, which means that the excretion of gadoxetic acid from HCC cells into the tumor blood spaces (tumor sinusoids) is enhanced, probably because of the depletion of bile ducts in HCCs. We surmise this to be a reactive response to the increase in OATP8 expression, to export more substrate into blood. In contrast, the excretion by MRP2, the transporter on the canalicular side, would not function in HCCs, because there are few larger bile ducts in tumor tissue. Therefore, the efflux of gadoxetic acid into tumor blood spaces would appear to be the main route of excretion from HCC cells in iso- or hyperintense HCCs. The rate of excretion is likely to be slower than the rate of uptake and thus to hardly influence the SI in the hepatobiliary phase of gadoxetic acid–enhanced MR imaging.

We also analyzed the histologic differences between hypointense HCCs and iso- or hyperintense HCCs. The majority of iso- or hyperintense HCCs were moderately differentiated HCCs; this may be due to genetic reversion to their original hepatocyte nature during hepatocarcinogenesis because, as shown by Tsuda et al (30), the ability of tumor cells to take up gadoxetic acid would be expected to be lost during the early stage of hepatocarcinogenesis in rats. Interestingly, iso- or hyperintense HCCs showed pseudoglandular proliferation

Figure 6

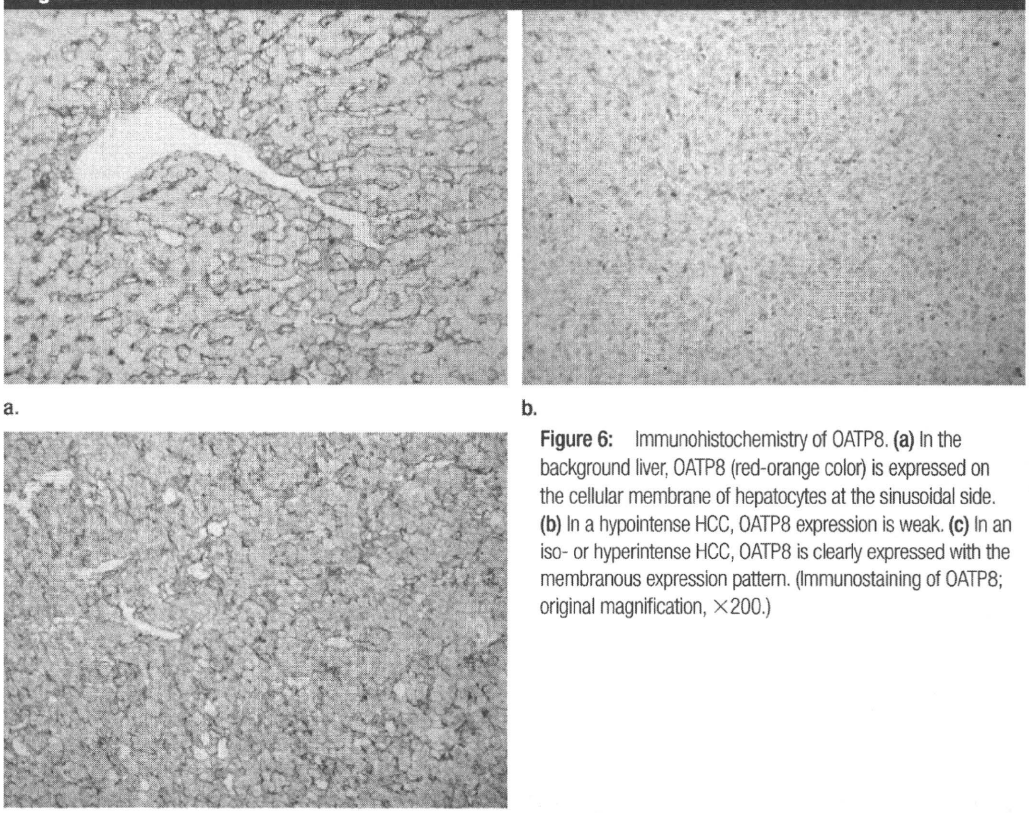

Figure 6: Immunohistochemistry of OATP8. **(a)** In the background liver, OATP8 (red-orange color) is expressed on the cellular membrane of hepatocytes at the sinusoidal side. **(b)** In a hypointense HCC, OATP8 expression is weak. **(c)** In an iso- or hyperintense HCC, OATP8 is clearly expressed with the membranous expression pattern. (Immunostaining of OATP8; original magnification, ×200.)

Figure 7

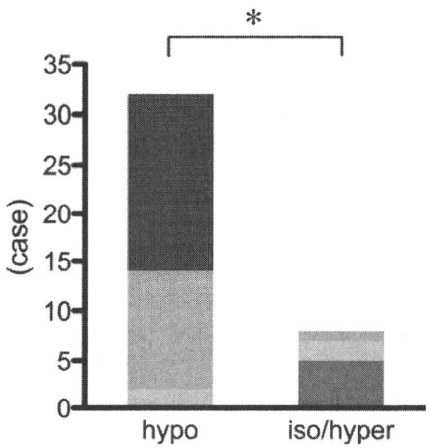

Figure 7: Bar graph shows results of semiquantitative analysis of the immunohistochemistry of OATP8. OATP8 expression in iso- or hyperintense HCCs *(iso/hyper)* is significantly extensive compared with that in hypointense HCCs *(hypo)* (* = $P < .001$, Mann-Whitney test). Blue = no expression, green = decreased expression, yellow = equivalent expression, red = increased expression.

with bile plugs with significantly high frequency, suggesting overproduction of bile and secondary dilatation of bile canaliculi (31). Overexpression of OATP8 might contribute to the overproduction of bile, because OATP8 can take up bile acid components. However, this proliferation pattern was also fairly often seen in hypointense HCCs. It is difficult to directly correlate the expression levels of OATP8 and the quantity of bile production, because nonanion transporters such as Na^+/taurocholate cotransporting polypeptide and organic cation transporter also participate in bile production (32).

Benign hepatocellular nodules, like focal nodular hyperplasia, commonly show isointensity or hyperintensity in the hepatobiliary phase (4–6). We suppose that uptake transporters, including OATP8 and export transporters, are expressed normally or increasingly in these hyperplastic cells. However, the SI may be determined by the expression of uptake transporters rather than that of export transporters, as shown in our study. Radiologic-pathologic studies of benign or premalignant hepatocellular nodules performed with similar methods are needed to clarify this issue.

Our study had several limitations. First, the total number of iso- or hyperintense HCCs examined was small because such tumors are relatively rare, and reverse transcription PCR was performed in only 22 of 40 HCCs from which we could obtain fresh-frozen specimens. Second, we simply divided HCCs into hypointense and iso- or hyperintense type according to the average SI in the maximum ROI for this analysis. In the future, it will be important to correlate each area of different SI with tumor differentiation, proliferation pattern, or the expression of transporters in heterogeneous lesions. However, we believe that the data obtained are sufficient to make conclusions about the molecular biology of gadoxetic acid–enhanced MR imaging pharmacodynamics, because the expression levels

Figure 8

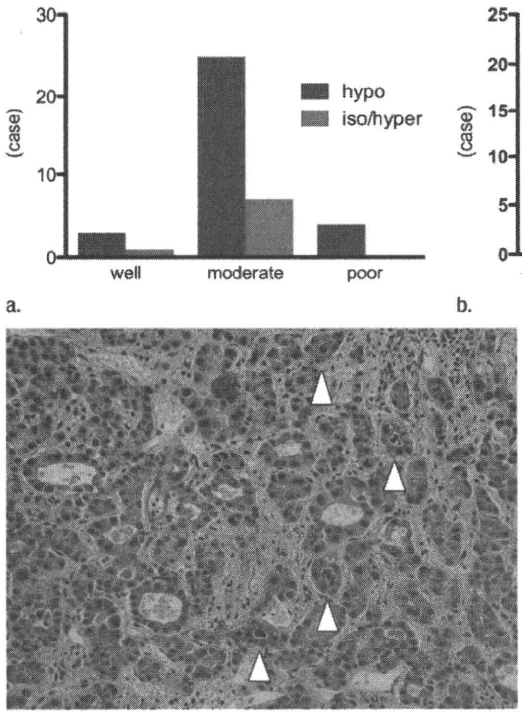

Figure 8: Histologic proliferation patterns of HCCs. **(a)** Graph shows tumor differentiation. The hypointense HCCs *(hypo)* consisted of well-differentiated (9%), moderately differentiated (78%), and poorly differentiated HCCs (12%), while 88% of iso- or hyperintense HCCs *(iso/hyper)* were moderately differentiated. **(b)** Graph shows tumor proliferation pattern. Seventy-five percent of iso- or hyperintense HCCs had a pseudoglandular pattern, and 88% showed bile plugs. In the hypointense HCCs, the trabecular pattern was most common; in addition, a pseudoglandular *(PG)* proliferation pattern and bile production were observed in 19% and 31% of nodules, respectively. There was no significant difference in tumor differentiation ($P = .57$), while there were significant differences in proliferation patterns or bile production between the two types of HCCs ($P = .01$ and $P = .006$, respectively). **(c)** A case of iso- or hyperintense HCC shows a pseudoglandular pattern with bile production (arrowheads). (Hematoxylin-eosin stain; original magnification, ×200.)

Figure 9

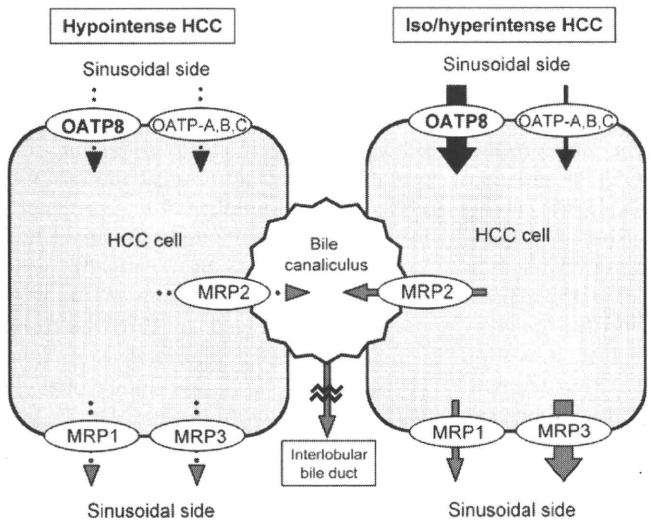

Figure 9: Schematic of transporter expression and mechanism of gadoxetic acid dynamics in HCC. Between hypointense and iso- or hyperintense HCCs, the most significant differences were observed in OATP8 and MRP3 expression. That is, in iso- or hyperintense HCCs, a larger amount of gadoxetic acid would be taken up from the tumor blood sinusoids into HCC cells by OATP8 and be excreted again into tumor blood sinusoids by MRP3 very gradually, probably because of the depletion of bile ducts in the HCCs. In contrast, in hypointense HCCs, the uptake of gadoxetic acid might be blocked or reduced because of the lower expression of OATP8.

of OATP8 and MRP3 and the time-SI curves showed significant differences between the two types of HCCs. Third, patients with poor liver function were not included in this study. The relative SI in the hepatobiliary phase would be modified in these patients; for example, HCC without OATP8 expression could be visualized as isointense. Therefore, the liver function of patients should be considered when evaluating the SI of HCCs (33,34).

In conclusion, the expression of the uptake transporter OATP8 and the export transporter MRP3 in HCC cells significantly correlated with the SI of HCCs in the hepatobiliary phase of gadoxetic acid–enhanced MR imaging. In human HCC cells, OATP8 and MRP3 are probably the uptake transporter and export transporter of gadoxetic acid, respectively.

References

1. Vogl TJ, Kümmel S, Hammerstingl R, et al. Liver tumors: comparison of MR imaging with Gd-EOB-DTPA and Gd-DTPA. Radiology 1996;200(1):59–67.

2. Huppertz A, Balzer T, Blakeborough A, et al. Improved detection of focal liver lesions at MR imaging: multicenter comparison

of gadoxetic acid-enhanced MR images with intraoperative findings. Radiology 2004; 230(1):266–275.

3. Bluemke DA, Sahani D, Amendola M, et al. Efficacy and safety of MR imaging with liver-specific contrast agent: U.S. multicenter phase III study. Radiology 2005;237(1):89–98.
4. Huppertz A, Haraida S, Kraus A, et al. Enhancement of focal liver lesions at gadoxetic acid-enhanced MR imaging: correlation with histopathologic findings and spiral CT—initial observations. Radiology 2005; 234(2):468–478.
5. Zech CJ, Herrmann KA, Reiser MF, Schoenberg SO. MR imaging in patients with suspected liver metastases: value of liver-specific contrast agent Gd-EOB-DTPA. Magn Reson Med Sci 2007;6(1):43–52.
6. Reimer P, Schneider G, Schima W. Hepatobiliary contrast agents for contrast-enhanced MRI of the liver: properties, clinical development and applications. Eur Radiol 2004; 14(4):559–578.
7. Saito K, Kotake F, Ito N, et al. Gd-EOB-DTPA enhanced MRI for hepatocellular carcinoma: quantitative evaluation of tumor enhancement in hepatobiliary phase. Magn Reson Med Sci 2005;4(1):1–9.
8. Schuhmann-Giampieri G, Schmitt-W llich H, Press WR, Negishi C, Weinmann HJ, Speck U. Preclinical evaluation of Gd-EOB-DTPA as a contrast agent in MR imaging of the hepatobiliary system. Radiology 1992;183(1):59–64.
9. Hamm B, Staks T, Mühler A, et al. Phase I clinical evaluation of Gd-EOB-DTPA as a hepatobiliary MR contrast agent: safety, pharmacokinetics, and MR imaging. Radiology 1995;195(3):785–792.
10. Hecht EM, Holland AE, Israel GM, et al. Hepatocellular carcinoma in the cirrhotic liver: gadolinium-enhanced 3D T1-weighted MR imaging as a stand-alone sequence for diagnosis. Radiology 2006;239(2):438–447.
11. Reimer P, Rummeny EJ, Daldrup HE, et al. Enhancement characteristics of liver metastases, hepatocellular carcinomas, and hemangiomas with Gd-EOB-DTPA: preliminary results with dynamic MR imaging. Eur Radiol 1997;7(2):275–280.
12. Bartolozzi C, Crocetti L, Lencioni R, Cioni D, Della Pina C, Campani D. Biliary and reticuloendothelial impairment in hepatocarcinogenesis: the diagnostic role of tissue-specific MR contrast media. Eur Radiol 2007; 17(10):2519–2530.
13. van Montfoort JE, Stieger B, Meijer DK, Weinmann HJ, Meier PJ, Fattinger KE. Hepatic uptake of the magnetic resonance imaging contrast agent gadoxetate by the organic anion transporting polypeptide Oatp1. J Pharmacol Exp Ther 1999;290(1): 153–157.
14. Lorusso V, Pascolo L, Fernetti C, Visigalli M, Anelli P, Tiribelli C. In vitro and in vivo hepatic transport of the magnetic resonance imaging contrast agent B22956/1: role of MRP proteins. Biochem Biophys Res Commun 2002;293(1):100–105.
15. Abe T, Kakyo M, Tokui T, et al. Identification of a novel gene family encoding human liver-specific organic anion transporter LST-1. J Biol Chem 1999;274(24): 17159–17163.
16. Hsiang B, Zhu Y, Wang Z, et al. A novel human hepatic organic anion transporting polypeptide (OATP2). Identification of a liver-specific human organic anion transporting polypeptide and identification of rat and human hydroxymethylglutaryl-CoA reductase inhibitor transporters. J Biol Chem 1999;274(52):37161–37168.
17. König J, Cui Y, Nies AT, Keppler D. Localization and genomic organization of a new hepatocellular organic anion transporting polypeptide. J Biol Chem 2000;275(30): 23161–23168.
18. Kullak-Ublick GA, Ismair MG, Stieger B, et al. Organic anion-transporting polypeptide B (OATP-B) and its functional comparison with three other OATPs of human liver. Gastroenterology 2001;120(2):525–533.
19. Kullak-Ublick GA, Hagenbuch B, Stieger B, et al. Molecular and functional characterization of an organic anion transporting polypeptide cloned from human liver. Gastroenterology 1995;109(4):1274–1282.
20. Vavricka SR, Jung D, Fried M, Grützner U, Meier PJ, Kullak-Ublick GA. The human organic anion transporting polypeptide 8 (SLCO1B3) gene is transcriptionally repressed by hepatocyte nuclear factor 3beta in hepatocellular carcinoma. J Hepatol 2004;40(2): 212–218.
21. Zhou SF, Wang LL, Di YM, et al. Substrates and inhibitors of human multidrug resistance associated proteins and the implications in drug development. Curr Med Chem 2008; 15(20):1981–2039.
22. Müller M, Roelofsen H, Jansen PL. Secretion of organic anions by hepatocytes: involvement of homologues of the multidrug resistance protein. Semin Liver Dis 1996;16(2): 211–220.
23. Tsujii H, König J, Rost D, Stöckel B, Leuschner U, Keppler D. Exon-intron organization of the human multidrug-resistance protein 2 (MRP2) gene mutated in Dubin-Johnson syndrome. Gastroenterology 1999; 117(3):653–660.
24. König J, Rost D, Cui Y, Keppler D. Characterization of the human multidrug resistance protein isoform MRP3 localized to the basolateral hepatocyte membrane. Hepatology 1999;29(4):1156–1163.
25. Zech CJ, Vos B, Nordell A, et al. Vascular enhancement in early dynamic liver MR imaging in an animal model: comparison of two injection regimen and two different doses Gd-EOB-DTPA (gadoxetic acid) with standard Gd-DTPA. Invest Radiol 2009;44(6): 305–310.
26. Terminology of nodular hepatocellular lesions. International Working Party. Hepatology 1995;22(3):983–993.
27. Hirohashi S, Ishak KG, Kojiro M, et al. Hepatocellular carcinoma. In: Hamilton SR, Aaltonen LA, eds. Pathology and genetics of tumours of the digestive system. Lyon, France: IARC, 2000; 157–172.
28. Nakamura K, Zen Y, Sato Y, et al. Vascular endothelial growth factor, its receptor Flk-1, and hypoxia inducible factor-1alpha are involved in malignant transformation in dysplastic nodules of the liver. Hum Pathol 2007;38(10):1532–1546.
29. Narita M, Hatano E, Arizono S, et al. Expression of OATP1B3 determines uptake of Gd-EOB-DTPA in hepatocellular carcinoma. J Gastroenterol 2009;44(7):793–798.
30. Tsuda N, Kato N, Murayama C, Narazaki M, Yokawa T. Potential for differential diagnosis with gadolinium-ethoxybenzyl-diethylenetriamine pentaacetic acid-enhanced magnetic resonance imaging in experimental hepatic tumors. Invest Radiol 2004;39(2):80–88.
31. Kondo Y, Nakajima T. Pseudoglandular hepatocellular carcinoma. A morphogenetic study. Cancer 1987;60(5):1032–1037.
32. Kullak-Ublick GA, Beuers U, Paumgartner G. Hepatobiliary transport. J Hepatol 2000; 32(1 suppl):3–18.
33. Ryeom HK, Kim SH, Kim JY, et al. Quantitative evaluation of liver function with MRI Using Gd-EOB-DTPA. Korean J Radiol 2004;5(4):231–239.
34. Kim T, Murakami T, Hasuike Y, et al. Experimental hepatic dysfunction: evaluation by MRI with Gd-EOB-DTPA. J Magn Reson Imaging 1997;7(4):683–688.

Cancer Science
The official journal of the Japanese Cancer Association JCA

Phase I/II study of the pharmacokinetics, safety and efficacy of S-1 in patients with advanced hepatocellular carcinoma

Junji Furuse,[1,2,6] Takuji Okusaka,[3] Shuichi Kaneko,[4] Masatoshi Kudo,[5] Kohei Nakachi,[1] Hideki Ueno,[3] Tatsuya Yamashita[4] and Kazuomi Ueshima[5]

[1]Hepatobiliary and Pancreatic Oncology Division, National Cancer Center Hospital East, Kashiwa; [2]Medical Oncology Division, Kyorin University School of Medicine, Mitaka-shi; [3]Hepatobiliary and Pancreatic Oncology Division, National Cancer Center Hospital, Tokyo; [4]Department of Gastroenterology, Kanazawa University Hospital, Kanazawa, Ishikawa; [5]Department of Gastroenterology and Hepatology, Kinki University School of Medicine, Osaka, Japan

(Received April 26, 2010/Revised August 17, 2010/Accepted August 18, 2010/Accepted manuscript online August 26, 2010/Article first published online October 14, 2010)

S-1, an oral fluoropyrimidine derivative, has been shown to be clinically effective against various solid tumors, and preclinical studies have demonstrated activity against hepatocellular carcinoma. We conducted a phase I/II study in patients with advanced hepatocellular carcinoma to examine the pharmacokinetics, recommended dose, safety and efficacy of S-1. In phase I, the administered dose of S-1 was approximately 64 mg/m^2 per day in three patients (level 1) and approximately 80 mg/m^2 per day in six patients (level 2). There was no dose-limiting toxicity at level 1, but two patients had dose-limiting toxicity at level 2 (grade 3 anorexia and grade 2 rash requiring eight or more consecutive days of rest). The recommended dose was finally estimated to be 80 mg/m^2 per day. There were no significant differences in the pharmacokinetics of S-1 between patients with Child-Pugh A and those with B. In phase II, five of 23 patients (21.7%) had partial responses. The median progression-free survival and overall survival were 3.7 and 16.6 months, respectively. The most common toxicities of grade 3 or 4 were elevated serum aspartate aminotransferase levels, hypochromia and thrombocytopenia. In conclusion, S-1 showed an acceptable toxicity profile and promising antitumor activity for hepatocellular carcinoma, warranting further evaluation in randomized clinical trials. (*Cancer Sci* 2010; 101: 2606–2611)

Hepatocellular carcinoma (HCC) is one of the most common cancers in the world. Outcomes remain poor because the disease is usually advanced and associated with hepatic impairment at diagnosis, and because of the high rate of recurrence resulting from either intrahepatic metastases from the primary tumor or multicentric lesions. As for therapy, surgical resection and percutaneous ethanol injection (PEI) or radiofrequency ablation (RFA) are considered the mainstays of treatment in patients with potentially curable disease. Transcatheter arterial chemoembolization (TACE) is the treatment of choice for noncurative HCC. Despite numerous clinical trials of a wide variety of cytotoxic agents, survival remains dismal in HCC.[1] Recently, sorafenib, an oral multi-kinase inhibitor that targets mainly Raf kinases and receptor tyrosine kinases associated with angiogenesis (vascular endothelial growth factor receptor [VEGFR]-2/-3 and platelet-derived growth factor receptor [PDGFR]-β), provided a significant survival benefit in patients with advanced HCC enrolled in placebo-controlled, randomized, phase III trials, including Asian as well as European subjects.[2,3] An initial phase I study in Japanese patients with HCC associated mainly with hepatitis C virus (HCV) infection showed promising antitumor activity and a favorable tolerability profile.[4] However, further improvement in the treatment of advanced HCC is essential.

S-1 is a novel, orally administered drug that combines tegafur (FT), 5-chloro-2,4-dihydroxypyridine (CDHP) and oteracil potassium (Oxo) in a molar concentration ratio of 1:0.4:1.[5] CDHP is a competitive inhibitor of dihydropyrimidine dehydrogenase (DPD), a metabolizing enzyme of 5-fluorouracil (5-FU) that is expressed in the liver. Inhibition of DPD by CDHP results in prolonged effective concentrations of 5-FU in plasma and tumor tissue.[6] Oxo, a competitive inhibitor of orotate phosphoribosyltransferase, inhibits the phosphorylation of 5-FU in the gastrointestinal tract, thereby reducing serious 5-FU-related gastrointestinal toxicity.[7] Clinically, S-1 has been shown to be effective against a variety of solid tumors, with response rates ranging 21–49% in late phase II studies conducted in Japan.[8] S-1 has yet to be evaluated in patients with HCC. However, in nude rats with human HCC xenografts, S-1 has been confirmed to have antitumor activity.[9]

Patients with HCC usually have various degrees of liver dysfunction because of associated liver disease and replacement of liver tissue by tumor, leading to pathophysiological changes that influence drug disposition. Decreased hepatic blood flow, extrahepatic and intrahepatic blood shunting and hepatocyte loss also alter drug metabolism, and decreased protein synthesis reduces drug binding to plasma proteins. In fact, the maximal tolerated dose (MTD) of 5-FU given as a 5-day continuous infusion in patients with HCC is approximately 50% of that in patients with normal organ function, and patients with cirrhosis have significantly lower clearance of 5-FU than those without cirrhosis.[10] We therefore conducted a multicenter phase I/II study to evaluate the pharmacokinetics, safety and efficacy of S-1 monotherapy in patients with advanced HCC.

Materials and Methods

Eligibility. Eligible patients had histologically or cytologically proved HCC that was not amenable to treatment by resection, liver transplantation, RFA, PEI or percutaneous microwave coagulation therapy (PMCT) and was not expected to respond to TACE. A hypervascular mass on computed tomography (CT) or magnetic resonance imaging (MRI) associated with a serum alpha-fetoprotein level or a serum protein induced by vitamin K absence or antagonist (PIVKA-II) level of more than the upper limit of normal (ULN) was considered a sufficient non-invasive diagnostic criterion for HCC. At least one measurable lesion on CT or MRI (not including necrotic lesions caused by prior treatment) was required. Other eligibility criteria included: age of at least 20 years; Eastern Cooperative Oncology Group (ECOG) performance status (PS) of 0–2; estimated life expectancy of at least 60 days; adequate

[6]To whom correspondence should be addressed. E-mail: jfuruse@ks.kyorin-u.ac.jp
Clinical trial registration: this trial was not registered in the clinical trial database because it was an early phase trial and not a controlled study.

doi: 10.1111/j.1349-7006.2010.01730.x

hematological function (white blood cells [WBC] ≥3000/mm^3, hemoglobin ≥ 9.0 g/dL, platelets ≥ 7.0 × 10^4/mm^3); adequate hepatic function (aspartate aminotransferase [AST] and alanine aminotransferase [ALT] ≤5 times the ULN, total bilirubin ≤2.0 mg/dL, serum albumin ≥2.8 g/dL, prothrombin activity ≥40%); adequate renal function (serum creatinine ≤ULN); and a Child-Pugh class of A or B. Prior treatment for HCC, such as resection, liver transplantation, RFA, PEI, PMCT and TACE was permitted if the treatment had been performed 30 or more days before registration in the study. Patients were excluded if they had: tumor involving more than 50% of the liver; brain or bone metastasis or vascular invasion of the main trunk and first-order branch(es) of the portal vein, hepatic veins, hepatic arteries or bile duct; severe complications; other malignancies; or inability to comply with the protocol requirements. Written informed consent was obtained from each patient. The study was approved by the local institutional review boards at all participating centers.

Study design. S-1 was supplied by Taiho Pharmaceutical Co., Ltd (Tokyo, Japan) in capsules containing 20 or 25 mg of FT. Individual doses were calculated according to body surface area. The calculated dose was rounded to derive the daily dose and the number of capsules to be dispensed per patient. At each dose level, S-1 was administered orally twice daily (after breakfast and dinner) for 28 consecutive days, followed by a 14-day recovery period. Each treatment cycle was 42 days. If grade 3 or higher hematological toxicity, grade 2 or higher non-hematological toxicity, grade 3 or higher elevations of AST or ALT, or grade 2 or higher increases in the serum creatinine concentration occurred, treatment with S-1 was temporarily suspended, the dose of S-1 was reduced, or both (minimum dose, 50 mg/day). Treatment continued until there was evidence of disease progression, or if the recovery period exceeded 28 days, the patient requested treatment to be discontinued or unacceptable toxicity developed and treatment was terminated at the discretion of the investigator. Drug compliance and accountability were carefully monitored; patients were requested to record their intake of S-1 and other medications in a diary.

During phase I, the starting dose of S-1 (level 1) was approximately 64 mg/m^2 per day twice daily (80% of the standard dose), level 2 was approximately 80 mg/m^2 per day and level 0 was approximately 50 mg/m^2 per day (80% of level 1). Patients were enrolled in cohorts of three for each dose level. The dose was escalated according to the cohort and was not increased in the same patient. If none of the first three patients had dose-limiting toxicity (DLT) during the first cycle, the dose was increased to level 2. If one or two of the first three patients had DLT, three additional patients were entered at the same dose level; if only one or two of the first six patients at level 1 had DLT, the dose was increased to level 2; if all of the first three patients or three or more of the first six patients had DLT, the dose was decreased to level 0; if none of the first three patients had DLT at level 0 or level 2, three additional patients were assigned to receive the same dose level. The DLT was defined as any of the following: (i) hematological toxicity ≥grade 4; (ii) non-hematological toxicity ≥grade 3; (iii) AST, ALT ≥15 times the ULN; or (iv) a rest period of 8 or more consecutive days was required. The recommended dose (RD) determined in the phase I part of this study was used in phase II.

Pharmacokinetics. Blood samples (5 mL) were obtained from each patient assigned to receive level 2 in the phase I part of the study. The samples were taken before and 1, 2, 4, 6, 8, 10 and 12 h after administration of S-1 on days 1 and 8 of the first treatment cycle. Plasma was separated from the whole-blood samples by centrifugation and stored at −20°C until analysis. Plasma FT concentrations were measured by high-performance liquid chromatography with ultraviolet detection. Plasma concentrations of 5-FU, CDHP and Oxo were measured by gas chromatography-negative ion chemical ionization mass spectrometry, as described previously.[11]

Pharmacokinetic data, including the maximum plasma concentration (C_{max}, ng/mL), time to reach C_{max} (T_{max}, h), area under the plasma-concentration–time curve for 0–12 h (AUC_{0-12}, ng h/mL) and the elimination half-life ($T_{1/2}$, h) were calculated by noncompartment model analysis using WinNonlin software, version 4.1 (Pharsight, Cary, NC, USA).

Assessment of efficacy and toxicity. All patients who received at least one dose of the study drug were included in the evaluations of response and toxicity. During each course of treatment, tumor response was assessed according to the Response Evaluation Criteria in Solid Tumors (RECIST) by computed tomography (CT) or magnetic resonance imaging (MRI), with a slice thickness of no more than 5 mM.[12] The primary efficacy end-point in the phase II part of this study was the overall response rate, assessed on the basis of changes in tumor dimensions. The other end-points were overall survival (OS) and progression-free survival (PFS). The PFS was defined as the interval between the date of initiating treatment and the date on which disease progression was first confirmed or the date of death from any cause. Overall survival was defined at the interval from the date of initiating treatment to the date of death from any cause. Median OS and median PFS were

Table 1. Patient characteristics

	Level 1 (*n* = 3)	Level 2 (*n* = 23)
	n (%)	*n* (%)
Median age (range) (years)	67.0 (63–68)	68.0 (45–78)
Gender		
Male	2 (66.7)	21 (91.3)
Female	1 (33.3)	2 (8.7)
Virus marker		
HBs (+)	1 (33.3)	3 (13.0)
HCV (+)	1 (33.3)	14 (60.9)
HBs(−), HCV(−)	1 (33.3)	6 (26.1)
Child-Pugh classification		
A	3 (100)	16 (69.6)
B	0 (0)	7 (30.4)
Stage		
Stage II	1 (33.3)	3 (13.0)
Stage III	1 (33.3)	10 (43.5)
Stage IVB	1 (33.3)	10 (43.5)
Vascular invasion	0 (0)	2 (8.7)
ECOG PS		
0	3 (100)	21 (91.3)
1	0 (0)	2 (8.7)
Pretreatment		
TA(C)E	2 (66.7)	17 (73.9)
Surgery	1 (33.3)	8 (34.8)
RFA	0 (0)	7 (30.4)
HAI	2 (66.7)	6 (26.1)
PEI	0 (0)	4 (17.4)
Radiation	0 (0)	4 (17.4)
PMCT	0 (0)	3 (13.0)
Systemic chemotherapy	0 (0)	3 (13.0)
BCLC staging		
Early	0 (0)	1 (4.3)
Intermediate	2 (66.7)	11 (47.8)
Advanced	1 (33.3)	11 (47.8)

BCLC, Barcelona Clinic Liver Cancer Group; ECOG, Eastern Cooperative Oncology Group; HAI, hepatic arterial infusion; HBs, hepatitis B surface antigen; HCV, hepatitis C virus antibody; PEI, percutaneous ethanol injection; PMCT, percutaneous microwave coagulation therapy; PS, performance status; RFA, radiofrequency ablation; TACE, transcatheter arterial chemoembolization.

Table 2. Toxic effects

Toxicity	Level 1 (n = 3)		Level 2 (n = 23)		Child Pugh A (n = 16)		Child Pugh B (n = 7)	
	All grades	≥G3	All grades	≥G3	All grades	≥G3	All grades	≥G3
	n (%)	n (%)	n (%)	n (%)	n (%)	n (%)	n (%)	n (%)
All adverse events	3 (100.0)	0 (0.0)	23 (100.0)	10 (43.5)	16 (100.0)	8 (50.0)	7 (100.0)	2 (28.6)
Hematological								
Erythropenia	1 (33.3)	0 (0.0)	21 (91.3)	1 (4.3)	14 (87.5)	1 (6.3)	7 (100.0)	0 (0.0)
Hypochromia	1 (33.3)	0 (0.0)	19 (82.6)	4 (17.4)	12 (75.0)	4 (25.0)	7 (100.0)	0 (0.0)
Leukopenia	2 (66.7)	0 (0.0)	18 (78.3)	1 (4.3)	12 (75.0)	1 (6.3)	6 (85.7)	0 (0.0)
Lymphopenia	2 (66.7)	0 (0.0)	12 (52.2)	3 (13.0)	7 (43.8)	3 (18.8)	5 (71.4)	0 (0.0)
Neutropenia	1 (33.3)	0 (0.0)	17 (73.9)	1 (4.3)	12 (75.0)	1 (6.3)	5 (71.4)	0 (0.0)
Reduced hematocrit	1 (33.3)	0 (0.0)	19 (82.6)	1 (4.3)	12 (75.0)	1 (6.3)	7 (100.0)	0 (0.0)
Reduced prothrombin content	1 (33.3)	0 (0.0)	19 (82.6)	0 (0.0)	14 (87.5)	0 (0.0)	5 (71.4)	0 (0.0)
Thrombocytopenia	1 (33.3)	0 (0.0)	18 (78.3)	4 (17.4)	12 (75.0)	4 (25.0)	6 (85.7)	0 (0.0)
Non-hematological								
Elevated alkaline phosphatase	0 (0.0)	0 (0.0)	8 (34.8)	1 (4.3)	7 (43.8)	1 (6.3)	1 (14.3)	0 (0.0)
Elevated lactate dehydrogenase	0 (0.0)	0 (0.0)	15 (65.2)	0 (0.0)	9 (56.3)	0 (0.0)	6 (85.7)	0 (0.0)
Elevated serum AST	1 (33.3)	0 (0.0)	8 (34.8)	4 (17.4)	6 (37.5)	3 (18.8)	2 (28.6)	1 (14.3)
Elevated serum bilirubin	0 (0.0)	0 (0.0)	18 (78.3)	3 (13.0)	13 (81.3)	2 (12.5)	5 (71.4)	1 (14.3)
Hyponatremic	0 (0.0)	0 (0.0)	8 (34.8)	0 (0.0)	5 (31.3)	0 (0.0)	3 (42.9)	0 (0.0)
Reduced cholinesterase	2 (66.7)	0 (0.0)	18 (78.3)	0 (0.0)	13 (81.3)	0 (0.0)	5 (71.4)	0 (0.0)
Reduced serum albumin	0 (0.0)	0 (0.0)	18 (78.3)	2 (8.7)	12 (75.0)	1 (6.3)	6 (85.7)	1 (14.3)
Reduced total protein	0 (0.0)	0 (0.0)	11 (47.8)	0 (0.0)	8 (50.0)	0 (0.0)	3 (42.9)	0 (0.0)
Anorexia	1 (33.3)	0 (0.0)	18 (78.3)	2 (8.7)	13 (81.3)	1 (6.3)	5 (71.4)	1 (14.3)
Ascites	0 (0.0)	0 (0.0)	7 (30.4)	0 (0.0)	3 (18.8)	0 (0.0)	4 (57.1)	0 (0.0)
Diarrhea	0 (0.0)	0 (0.0)	10 (43.5)	0 (0.0)	8 (50.0)	0 (0.0)	2 (28.6)	0 (0.0)
Fatigue	0 (0.0)	0 (0.0)	19 (82.6)	2 (8.7)	13 (81.3)	2 (12.5)	6 (85.7)	0 (0.0)
Pigmentation	0 (0.0)	0 (0.0)	20 (87.0)	0 (0.0)	14 (87.5)	0 (0.0)	6 (85.7)	0 (0.0)
Rash	0 (0.0)	0 (0.0)	8 (34.8)	0 (0.0)	5 (31.3)	0 (0.0)	3 (42.9)	0 (0.0)
Stomatitis	0 (0.0)	0 (0.0)	7 (30.4)	0 (0.0)	5 (31.3)	0 (0.0)	2 (28.6)	0 (0.0)

Dosage level, level 1, 2 (n = 3, 23); AST, aspartate aminotransferase.

Table 3. Efficacy in patients who received dose level 2

	Child-Pugh A (n = 16)	Child-Pugh B (n = 7)	Total (n = 23)
Partial response†	4	1	5
Stable disease‡	5	2	7
Progressive disease	7	3	10
Not evaluable	0	1	1
Response rate (90%CI)§ (%)	–	–	23.1 (9.0–40.4)
Response rate (95%CI) (%)	25.0 (7.3–52.4)	14.3 (0.4–57.9)	23.1 (7.5–43.7)
Median PFS (95% CI) (months)	3.3 (2.3–5.1)	3.7 (2.5–7.4)	3.7 (2.5–5.1)
Median OS (95% CI) (months)	17.8 (14.0–NA)	14.5 (9.6–18.7)	16.6 (14.0–24.5)
1-year survival (95% CI) (%)	–	–	69.6 (50.8–88.4)
1.5-years survival (95% CI) (%)	–	–	43.0 (22.6–63.5)
Disease control rate¶			
6W (95% CI) (%)	–	–	47.8 (26.8–69.4)
12W (95% CI) (%)	–	–	26.1 (10.2–48.4)
24W (95% CI) (%)	–	–	21.7 (7.5–43.7)

†Partial response was re-evaluated after at least 4 weeks in patients with a partial response. ‡Stable disease was reassessed after at least 6 weeks. §Response rate (90% CI) is a primary end-point. ¶Disease control rates were respectively estimated by dividing the number of patients with no disease progression by the total number of patients. Disease control was defined as a response of complete response, partial response or stable disease. CI, confidence interval; NA, not available; OS, overall survival; PFS, progression-free survival.

estimated using the Kaplan–Meier method. Physical findings and the results of serum chemical and urine analyses were assessed at 2-week intervals; vital signs were assessed as necessary. Patients were observed until death or at least 1 year after registration to determine survival status. The severity of all adverse events was evaluated according to the Common Terminology Criteria for Adverse Events, version 3.0 (CTCAE, Ver. 3.0). The duration of all adverse events and their relation to S-1 were initially assessed by the attending physicians. Subsequently, an independent review committee reviewed data on objective response and adverse events.

Statistical considerations. With the response rate as the primary end-point, a total sample size of at least 23 patients was estimated to be required in the phase II portion to allow the

doi: 10.1111/j.1349-7006.2010.01730.x

study to have a one-sided 5% significance level of 0.05 and a power of 70%, assuming a threshold response rate of 5% and an expected response rate of 20%.

Results

Patient characteristics and treatment. Between May 2006 and April 2007, a total of 26 patients (nine in phase I and 17 in phase II) were enrolled at four centers in Japan. All patients were eligible for the evaluation of toxicity and efficacy. The first six patients who received dose level 2 (80 mg/m^2 per day) during the phase I part of this study were included in the phase II assessment, along with the 17 other patients (a total of 23 patients in the phase II assessment). The characteristics of patients are summarized in Table 1. At the study entry, 11 of 26 (42.3%) had metastatic disease. Six patients (23.1%) had single extrahepatic metastases (lung metastases, three patients; lymph node metastasis, three patients). Four patients had two sites of metastases, including the lung, lymph nodes and adrenal glands. Of the 26 patients, 23 had received some prior treatment, including three who had received systemic chemotherapy.

Dose-limiting toxicity and RD. None of the three patients who received dose level 1 (64 mg/m^2 per day) in the phase I part of the study had DLT. At dose level 2 (80 mg/m^2 per day), one patient with Child-Pugh class B had grade 3 anorexia during the first course of treatment, but the other two patients in the same cohort had no DLT. Three additional patients were enrolled to confirm safety, and one patient with Child-Pugh class B had a grade 2 rash; recovery required eight or more consecutive days of rest. Because two of the six patients who received level 2 had DLT, level 2 was defined as the RD for the phase II part of the study.

Treatment delivered. Twenty-three patients received a total of 85 cycles of treatment at dose level 2 (median, three cycles per patient; range, 1–15). The dose of S-1 was reduced in seven patients (30.4%) or a total of nine cycles (10.6%). The most common reasons for dose reductions were rash in four patients, and elevated serum bilirubin concentrations and anorexia in two patients each (some overlap among patients). Treatment was delayed because of toxicity in 12 patients (20 cycles), most often in cycles 1 or 2. The most common reasons for toxicity-related treatment delays were fatigue (five patients), rash (four patients) and elevated serum bilirubin concentrations (three patients). The reasons for terminating treatment were progressive disease in 19 patients (82.6%), adverse reactions in two patients (8.7%) and other reasons in two patients (8.7%; one required 28 or more consecutive days of rest, and one withdrew consent).

Toxicity. Drug-related adverse events occurring in all 26 patients in the phase I/II portion of the study are shown in Table 2. Treatment with S-1 was generally well tolerated throughout the study. Grade 3 or 4 toxicity occurred in 10 of the 23 patients (43.5%) who received level 2. Most toxic effects were laboratory abnormalities. There was no grade 3 or 4 toxicity at level 1. The most common grade 3 or 4 hematological toxic effects were hypochromia (17.4%), thrombocytopenia (17.4%) and lymphopenia (13.0%); the most common grade 3 or 4 nonhematological toxic effects were elevated serum AST levels (17.4%) and elevated serum bilirubin concentrations (13.0%).

Efficacy. A response could be evaluated in 26 patients in the phase I/II portion of the study. In the phase I part of the study (dose level 1), one patient had a partial response, one had progressive disease and the other was not evaluable. Of the 23 patients in the phase II part of the study, five (21.7%; 90% confidence interval [CI], 9.0–40.4%) responded to treatment Among the 23 patients in whom a response could be evaluated, five had a partial response, seven had stable disease, and 10 had progressive disease (Table 3). The remaining patient underwent imaging studies, but treatment was completed after one course, and continuation of stable disease for at least 6 weeks could not be

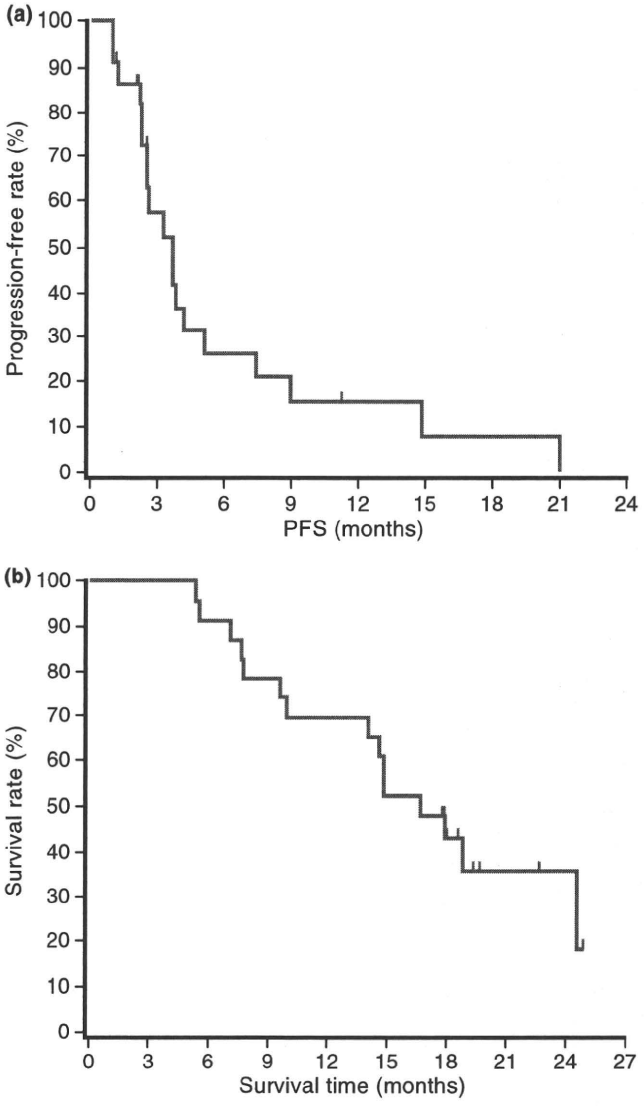

Fig. 1. Progression-free survival (PFS) (a) and overall survival (b) in patients who received dose level 2 of S-1 (n = 23). The median progression-free survival and overall survival were 3.7 and 16.6 months, respectively.

Table 4. Pharmacokinetics of FT, 5-FU, CDHP and Oxo on day 1 and day 8 in patients with HCC who received dose level 2

		C_{max} (ng/mL)	T_{max} (h)	AUC_{0-12} (ng h/mL)	$T_{1/2}$ (h)
FT	Day 1	2032 ± 437	3.3 ± 1.0	17070 ± 5139	10.1 ± 2.8
	Day 8	4365 ± 1712	3.7 ± 0.8	42399 ± 18137	12.7 ± 5.0
5-FU	Day 1	114.5 ± 35.5	4.3 ± 0.8	695.3 ± 223.6	2.3 ± 1.0
	Day 8	145.8 ± 31.4	4.3 ± 0.8	936.6 ± 292.3	2.4 ± 1.0
CDHP	Day 1	267.2 ± 76.8	3.3 ± 1.0	1424.8 ± 414.2	3.3 ± 0.9
	Day 8	281.0 ± 113.8	3.3 ± 1.0	1694.4 ± 603.5	3.4 ± 0.9
Oxo	Day 1	38.5 ± 1.8	3.7 ± 0.8	231.6 ± 69.8	4.0 ± 2.1
	Day 8	33.4 ± 9.5	4.0 ± 0.0	241.5 ± 115.6	4.0 ± 2.0

Parameters are represented as mean ± SD. CDHP, 5-chloro-2,4-dihydroxypyridine; 5-FU, 5-fluorouracil; FT, tegafur; Oxo, oteracil potassium.

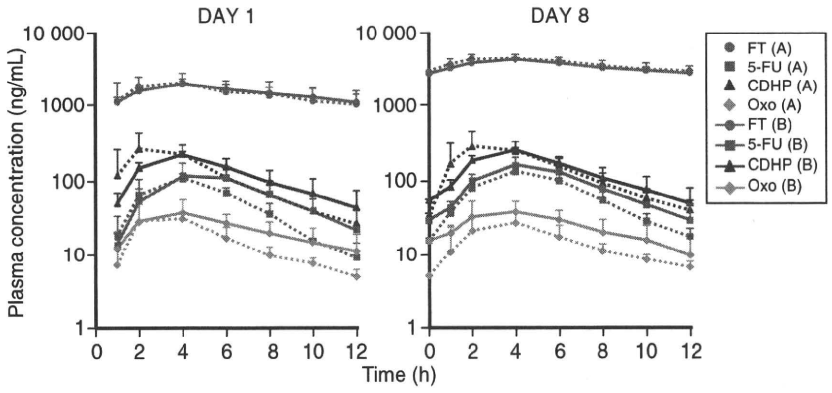

Fig. 2. Plasma-concentration–time profiles of tegafur (FT), 5-fluorouracil (5-FU), 5-chloro-2,4-dihydroxypyridine (CDHP) and oteracil potassium (Oxo) on day 1 and day 8 were similar in patients with Child-Pugh class A ($n = 3$) and those with Child-Pugh class B ($n = 3$).

confirmed. The duration of the five responses was 42, 147, 188, 238 and 371 days, respectively.

The median PFS was 3.7 months (95% CI, 2.5–5.1 months). The disease control rates at 6, 12 and 24 weeks were 47.8% (95% CI, 26.8–69.4%), 26.1% (95% CI, 10.2–48.4%) and 21.7% (95% CI, 7.5–43.7%), respectively. The PFS and OS are shown in Figure 1. The median OS was 16.6 months (95% CI, 14.0–24.5 months). Survival rates were 69.6% (95% CI, 50.8–88.4%) at 1 year and 43.0% (95% CI, 22.6–63.5%) at 1.5 years.

Pharmacokinetic analysis. Table 4 shows the pharmacokinetic data for the components of S-1 and 5-FU at level 2 on days 1 and 8. Compared with day 1, the C_{max} and $AUC_{0\text{-}12}$ of FT increased markedly on day 8; however, these increases were within the expected range given the slow elimination of FT, and repeated administration of S-1 had no effect on the T_{max} or $T_{1/2}$ of FT. There was no evidence of accumulation of 5-FU, CDHP or Oxo on day 8.

Figure 2 compares the plasma-concentration–time profiles of S-1 components and 5-FU between patients with Child-Pugh class A and those with Child-Pugh class B on days 1 and 8. The plasma-concentration–time profiles of FT, 5-FU, CDHP and Oxo were similar in patients with Child-Pugh class A and those with Child-Pugh class B on both days.

Discussion

There has been no established standard therapy for patients with advanced HCC refractory to surgery, transplantation, local ablation and TACE.[13,14] Some cytotoxic regimens have produced encouraging response rates, but survival benefits have been minimal compared with control groups, at the cost of clinically unacceptable adverse effects.[1,15]

S-1 is an anticancer drug consisting of FT, CDHP and Oxo. The conversion of FT to 5-FU is mediated mainly by hepatic cytochrome CYP2A6.[16] 5-FU is rapidly metabolized by DPD in the liver after the intravenous administration of 5-FU alone, but S-1, which includes a DPD inhibitor (i.e. CDHP), produces prolonged, effective concentrations of 5-FU in the blood. Thus, the liver plays an important role in the metabolism of FT.

The RD of S-1 in patients with HCC was estimated to be 80 mg/m^2 per day in phase I, which is similar to the dose recommended for the treatment of other solid tumors. However, in patients with HCC, Ueno *et al.*[10] reported that the DLT of 5-FU administered as a 5-day continuous infusion was stomatitis. Moreover, the MTD was equivalent to approximately 50% of that of 5-FU in patients with normal organ function,[10] suggesting that 5-FU-related gastrointestinal toxicity was reduced by Oxo in the formulation of S-1. We did not determine the MTD in this study because S-1 was approved for the treatment of other cancers. The pharmacokinetic properties of S-1 components and 5-FU in patients with HCC were similar to those in patients with pancreatic cancer or biliary tract cancer.[17,18]

Hematological toxic effects and symptomatic events such as pigmentation (87.0%), fatigue (82.6%), anorexia (78.3%) and ascites (30.4%) were more common than previously reported for S-1 in patients with other cancers. Nonetheless, severe toxic effects were comparable among patients with HCC and those with other cancers. Nonhematological toxic effects related to hepatic function were also more frequent than reported previously for S-1 in patients with other types of cancer, but such effects may have been caused by differences in underlying liver disease.

The pharmacokinetics of S-1 did not obviously differ between patients with Child-Pugh class A and those with Child-Pugh class B, suggesting that hepatic dysfunction associated with Child-Pugh class B did not affect the pharmacokinetics of S-1 components or 5-FU. The sample size of the pharmacokinetic evaluations was small because the primary end-point was to determine the RD as the evaluation of DLT in phase I. At dose level 2, DLT occurred in two patients with Child-Pugh class B (Grade 3 anorexia in one, and a Grade 2 rash requiring 8 or more consecutive days of rest in the other). There was no DLT at level 1 (given only to patients with Child-Pugh class A). However, the patient who had DLT of grade 3 anorexia had renal dysfunction at baseline, and the plasma 5-FU concentrations in this patient on day 8 were higher than those in other patients, perhaps contributing to the development of DLT (data not shown). In addition, there were no obvious differences in the incidence or grade of drug-related adverse events between patients with Child-Pugh class A and those with Child-Pugh class B, consistent with the results of pharmacokinetic analysis. These results suggested that there were no clinically meaningful differences in pharmacokinetics or safety according to Child-Pugh class or between patients with HCC and those with other cancers, and that S-1 was well tolerated in patients with HCC, similar to patients with other cancers. However, our study had several limitations: only a very small number of patients with Child-Pugh class B were included; among the patients with Child-Pugh class B, the score was heterogeneous, ranging from 7 to 9; and only patients with better scores were studied. Therefore, extra care should be taken when S-1 is given to patients with Child-Pugh class B.

As for efficacy, five of 23 patients had partial responses at dose level 2. Compared with previously reported response rates obtained with single-agent chemotherapy in patients with HCC, our results are good. In particular, the median OS appeared to be longer than that obtained with other agents in non-Japanese studies. The reason for the better OS in Japanese patients might be similar to that previously reported for sorafenib.[4] The median OS in our study was similar to that in a Japanese phase I study of sorafenib.[4] In studies of sorafenib in non-Japanese and

doi: 10.1111/j.1349-7006.2010.01730.x

Japanese patients with HCC, the median TTP and response rates were comparable, but the median OS was 15.6 months in Japanese patients compared with only 9.2 months in non-Japanese patients.[4] Differences in various treatments, including hepatic arterial infusion chemotherapy, and the palliative care of patients with progressive disease who had conditions such as hepatic decompression and variceal bleeding might be related to the longer survival time in Japanese rather than non-Japanese patients with HCC.

In conclusion, our results suggested that S-1 is effective and has an acceptable toxicity profile in patients with advanced HCC. Nonetheless, S-1 should be used with caution in the presence of liver dysfunction. Sorafenib has been established to be a standard treatment for advanced HCC. Perhaps, systemic chemotherapy with S-1 plus molecular-targeted therapies such as sorafenib will further improve survival in patients with advanced HCC or monotherapy with S-1 will be useful as a second-line regimen for chemotherapy.

Acknowledgments

We thank Drs T. Taguchi, M. Kurihara, K. Tanaka and K. Aiba for their kind advice, and Drs N. Moriyama, J. Tanaka and W. Koizumi for their extramural review. The authors are indebted to Peter Star of Medical Network K.K., Tokyo, Japan for his review of this manuscript. This study was supported by Taiho Pharmaceutical Co., Ltd.

Disclosure Statement

J. Furuse received honoraria for lecture fees from Taiho Pharmaceutical; T. Okusaka, S. Kaneko, M. Kudo, K. Nakachi, H. Ueno, T. Yamashita and K. Ueshima have no conflict of interest.

References

1 Zhu AX. Systemic therapy of advanced hepatocellular carcinoma: how hopeful should we be? *Oncologist* 2006; **11**: 790–800.
2 Cheng AL, Kang YK, Chen Z *et al.* Efficacy and safety of sorafenib in patients in the Asia-Pacific region with advanced hepatocellular carcinoma: a phase III randomised, double-blind, placebo-controlled trial. *Lancet Oncol* 2009; **10**: 25–34.
3 Llovet JM, Ricci S, Mazzaferro V *et al.* Sorafenib in advanced hepatocellular carcinoma. *N Engl J Med* 2008; **359**: 378–90.
4 Furuse J, Ishii H, Nakachi K, Suzuki E, Shimizu S, Nakajima K. Phase I study of sorafenib in Japanese patients with hepatocellular carcinoma. *Cancer Sci* 2008; **99**: 159–65.
5 Shirasaka T, Shimamato Y, Ohshimo H *et al.* Development of a novel form of an oral 5-fluorouracil derivative (S-1) directed to the potentiation of the tumor selective cytotoxicity of 5-fluorouracil by two biochemical modulators. *Anticancer Drugs* 1996; **7**: 548–57.
6 Tatsumi K, Fukushima M, Shirasaka T, Fujii S. Inhibitory effects of pyrimidine, barbituric acid and pyridine derivatives on 5-fluorouracil degradation in rat liver extracts. *Jpn J Cancer Res* 1987; **78**: 748–55.
7 Shirasaka T, Shimamoto Y, Fukushima M. Inhibition by oxonic acid of gastrointestinal toxicity of 5-fluorouracil without loss of its antitumor activity in rats. *Cancer Res* 1993; **53**: 4004–9.
8 Shirasaka T. Development history and concept of an oral anticancer agent S-1 (TS-1): its clinical usefulness and future vistas. *Jpn J Clin Oncol* 2009; **39**: 2–15.
9 Yamashita T, Kaneko S, Furuse J, *et al. Experimental and Early Clinical Studies of S-1, a Novel Oral DPD Inhibitor, Chemotherapy for Advanced Hepatocellular Carcinoma*. San Francisco: The American Association for the Study of Liver Diseases, 2008; Publication Number 1442.
10 Ueno H, Okada S, Okusaka T, Ikeda M, Kuriyama H. Phase I and pharmacokinetic study of 5-fluorouracil administered by 5-day continuous infusion in patients with hepatocellular carcinoma. *Cancer Chemother Pharmacol* 2002; **49**: 155–60.
11 Matsushima E, Yoshida K, Kitamura R, Yoshida K. Determination of S-1 (combined drug of tegafur, 5-chloro-2,4-dihydroxypyridine and potassium oxonate) and 5-fluorouracil in human plasma and urine using high-performance liquid chromatography and gas chromatography-negative ion chemical ionization mass spectrometry. *J Chromatogr B Biomed Sci* 1997; **691**: 95–104.
12 Therasse P, Arbuck SG, Eisenhauer EA *et al.* New guidelines to evaluate the response to treatment in solid tumors. European Organization for Research and Treatment of Cancer, National Cancer Institute of the United States, National Cancer Institute of Canada. *J Natl Cancer Inst* 2000; **92**: 205–16.
13 Couto OF, Dvorchik I, Carr BI. Causes of death in patients with unresectable hepatocellular carcinoma. *Dig Dis Sci* 2007; **52**: 3285–9.
14 Ng KK, Poon RT, Lo CM, Yuen J, Tso WK, Fan ST. Analysis of recurrence pattern and its influence on survival outcome after radiofrequency ablation of hepatocellular carcinoma. *J Gastrointest Surg* 2008; **12**: 183–91.
15 Thomas M. Molecular targeted therapy for hepatocellular carcinoma. *J Gastroenterol* 2009; **44**: 136–41.
16 Ikeda K, Yoshisue K, Matsushima E *et al.* Bioactivation of tegafur to 5-fluorouracil is catalyzed by cytochrome P-450 2A6 in human liver microsomes in vitro. *Clin Cancer Res* 2000; **6**: 4409–15.
17 Ueno H, Okusaka T, Ikeda M, Takezako Y, Morizane C. Phase II study of S-1 in patients with advanced biliary tract cancer. *Br J Cancer* 2004; **91**: 1769–74.
18 Ueno H, Okusaka T, Ikeda M, Takezako Y, Morizane C. An early phase II study of S-1 in patients with metastatic pancreatic cancer. *Oncology* 2005; **68**: 171–8.

Genomics 95 (2010) 217–223

Contents lists available at ScienceDirect

Genomics

journal homepage: www.elsevier.com/locate/ygeno

Comprehensive gene expression analysis of 5′-end of mRNA identified novel intronic transcripts associated with hepatocellular carcinoma

Yuji Hodo [a], Shin-ichi Hashimoto [b], Masao Honda [a], Taro Yamashita [a], Yutaka Suzuki [c], Sumio Sugano [c], Shuichi Kaneko [a,*], Kouji Matsushima [b]

[a] Department of Gastroentelorogy, Kanazawa University Graduate School of Medical Science, 13-1 Takara-Machi, Kanazawa, Ishikawa 920-8641, Japan
[b] Department of Molecular Preventive Medicine, School of Medicine, The University of Tokyo, 7-3-1, Hongo, Bunkyo-ku, Tokyo 113-0033, Japan
[c] Department of Medical Genome Sciences, Graduate School of Frontier Sciences, The University of Tokyo, 5-1-5, Kashiwanoha, Kashiwa, Chiba 277-8562, Japan

ARTICLE INFO

Article history:
Received 1 June 2009
Accepted 14 January 2010
Available online 21 January 2010

Keywords:
5′-end serial analysis of gene expression
Transcriptional start site
Acyl-coenzyme A oxidase 2
Intron
Hepatocellular carcinoma

ABSTRACT

To elucidate the molecular feature of human hepatocellular carcinoma (HCC), we performed 5′ end serial analysis of gene expression (5′SAGE), which allows genome wide identification of transcription start sites in addition to quantification of mRNA transcripts. Three 5′SAGE libraries were generated from normal human liver (NL), non B, non C HCC tumor (T), and background non tumor tissues (NT). We obtained 226,834 tags from these libraries and mapped them to the genomic sequences of a total of 8,410 genes using RefSeq database. We identified several novel transcripts specifically expressed in HCC including those mapped to the intronic regions. Among them, we confirmed the transcripts initiated from the introns of a gene encoding acyl coenzyme A oxidase 2 (*ACOX2*). The expression of these transcript variants were up regulated in HCC and showed a different pattern compared with that of ordinary *ACOX2* mRNA. The present results indicate that the transcription initiation of a subset of genes may be distinctively altered in HCC, which may suggest the utility of intronic RNAs as surrogate tumor markers.

Introduction

Hepatocellular carcinoma (HCC) is the fifth most common cancer worldwide and the third most common cause of cancer mortality. HCC usually develops in patients with virus induced (e.g., hepatitis B virus (HBV) and hepatitis C virus (HCV)) chronic inflammatory liver disease [1]; however, non B, non C HCC has been reported in patients negative for both HBV and HCV [2]. HCC development is a multistep process involving changes in host gene expression, some of which are correlated with the appearance and progression of a tumor. Multiple studies linking hepatitis viruses and chemical carcinogens with hepatocarcinogesis have provided insights into tumorigenesis [1,3]. Nevertheless, the genetic events that lead to HCC development remain unknown, and the molecular pathogenesis of HCC in most patients is still unclear. Therefore, elucidation of the genetic changes specific to the pathogenesis of non B, non C HCC may be useful to reveal the molecular features of HCCs irrelevant to viral infection.

Gene expression profiling, either by cDNA microarray [4] or serial analysis of gene expression (SAGE) [5], is a powerful molecular technique that allows analysis of the expression of thousands of genes. In particular, SAGE enables the rapid, quantitative, and simultaneous monitoring of the expression of tens of thousands of genes in various tissues [6,7]. Although numerous studies using cDNA microarrays and SAGE have been performed to clarify the genomic and molecular alterations associated with HCC [6,8 10], most expression data have been derived from the 3′ end region of mRNA. Recent advances in molecular biology have enabled genome wide analysis of the 5′ end region of mRNA that revealed the variation in transcriptional start sites [11,12] and the presence of a large number of non coding RNAs [13]. These approaches might be useful for identifying the unique and undefined genes associated with HCC not identified by the analysis of the 3′ end region of mRNA. SAGE based on the 5′ end (5′SAGE), a recently developed technique, allows for a comprehensive analysis of the transcriptional start site and quanti tative gene expression [14]. This article is to elucidate the molecular carcinogenesis of non B, non C HCCs, while those heterogeneous entities are supposed not to share the same etiology, by using 5′SAGE.

Results

Annotation of the 5′SAGE tags to the human genome

We characterized a total of 226,834 tags from three unique 5′SAGE libraries (75,268 tags from the normal liver (NL) library, 75,573 tags from the non tumor tissue (NT) library, and 75,993 tags from the tumor (T) library) and compared them against the human genome

Abbreviations: 5′SAGE, 5′-end serial analysis of gene expression; HCC, hepatocellular carcinoma; ACOX2, acyl-coenzyme A oxidase 2.

* Corresponding author. Fax: +81 76 234 4250
E-mail address: skaneko@m-kanazawa.jp (S. Kaneko).

0888-7543/$ – see front matter © 2010 Elsevier Inc. All rights reserved.
doi:10.1016/j.ygeno.2010.01.004

sequence. A total of 211,818 tags matched genomic sequences, representing 104,820 different tags in the three libraries (Table 1). About 60 65% of these tags mapped to a single locus in the genome in each library. Then, we mapped these single matched tags to the well annotated genes using RefSeq database (www.ncbi.nlm.nih.gov/RefSeq/, reference sequence database developed by NCBI). A total of 45,601 tags from the NL library, 39,858 from the NT library, and 41,265 from the T library were successfully mapped to 8410 unique genes (4397 genes detected in the NL library, 5194 genes in the NT library, and 6304 genes in the T library).

Gene expression profiling of non B, non C HCC

Abundantly expressed transcripts in the NL library and their corresponding expression in the NT and T libraries are shown in Table 2. The most abundant transcript in all three libraries was encoded by the *albumin (ALB)* gene. Transcripts encoding apolipoproteins were also abundantly expressed in each library, suggesting the preservation of hepatocytic gene expression patterns in HCC. Of note, the expression of *haptoglobin (HP)* (NL: 631, NT: 329, T: 57) and *metallothionein 1G (MT1G)* (NL: 392, NT: 169, T: 2) was decreased in the NT library and more in T library compared with NL library. Furthermore, the expression of *metallothionein 2A (MT2A)* (NL: 1027, NT: 872, T: 19), *metallothionein 1X (MT1X)* (NL: 547, NT: 644, T: 11), and *metallothionein 1E (MT1E)* (NL: 275, NT: 340, T: 2) was decreased almost fifty fold or more in the T library compared with the NL and NT libraries. In contrast, the expression of *ribosomal protein S29 (RPS29)* (NL: 372, NT: 1011, T: 1768) was increased in the NT library and more in T library compared with NL library. Thus, transcripts associated with a certain liver function including xenobiotic metabolism might be suppressed whereas those associated with protein synthesis might be expressed in non B, non C HCC, similar to that observed in HCV HCC [15].

We then investigated the characteristics of gene expression patterns in non B, non C HCC. Two hundred fifty four and 172 genes were up or down regulated in the T library more than five fold compared with the NL library (data not shown). The top 10 genes are listed in Table 3a, and we identified several novel genes not yet reported to be differentially expressed in non B, non C HCC. Representative novel gene expression changes identified by 5′SAGE were validated by semi quantitative reverse transcriptase polymerase chain reaction (RT PCR) analysis (Supplemental Fig. 1). RT PCR results showed that the expression of *galectin 4 (LGALS4)*, *X antigen family, member 1A (XAGE 1A)*, *retinol dehydrogenase 11 (RDH11)*, *hydroxysteroid (17 beta) dehydrogenase 14 (HSD17B14)*, *transmembrane 14A (TMEM14A)*, *stimulated by retinoic acid 13 homolog (STRA13)*, and *dual specificity phosphatase 23 (DUSP23)* was increased, whereas the expression of *C type lectin superfamily 4 member G (CLEC4G)* was decreased in HCC tissues compared with the non tumor tissues.

To further characterize the gene expression patterns of non B, non C HCC comprehensively, we compared the Gene Ontology process of three types of HCCs (i.e., non B, non C HCC; HBV HCC; HCV HCC) based on our previously described data [16]. The pathway analysis using MetaCore™ software showed that the immune related and cell adhesion related pathways were up regulated in HCV HCC with statistically significance, and the insulin signaling and angiogenesis related pathways were up regulated in HBV HCC with statistically significance, confirming our previous results [16]. Interestingly, genes associated with progesterone signaling were up regulated in non B, non C HCC, while genes associated with proteolysis in the cell cycle, apoptosis and the ESR1 nuclear pathway were up regulated in all types of HCC (Supplemental Fig. 2).

Dynamic alteration of transcription initiation in HCC

Although various transcriptome analyses have discovered considerable gene expression changes in cancer, it is still unclear if transcription is differentially initiated and/or terminated in HCC compared with the non cancerous liver. We therefore explored the characteristics of transcription initiation and/or termination in HCC using 5′SAGE and 3′SAGE data. Markedly, we observed relevant differences between 5′SAGE and 3′SAGE data derived from the same HCC sample (Tables 3a and b). For example, a gene encoding *coagulation factor XIII, B polypeptide (F13B)* was 13 fold up regulated at transcription start sites (5′SAGE) but two fold down regulated at transcription termination sites (3′SAGE). On the other hand, a gene encoding *adenylate cyclase 1 (ADCY1)* was 50 fold down regulated at transcriptional termination sites (3′SAGE) but showed no difference at transcriptional start sites (5′SAGE). These data suggest the dramatic alteration of all process of transcription in HCC, and the transcripts initiated at certain sites might be specifically associated with and involved in HCC pathogenesis, which could be a novel marker for HCC diagnosis.

Identification of novel intronic transcripts in HCC

Recent lines of evidence suggest that the majority of sequences of eukaryotic genomes may be transcribed, not only from known transcription start sites but also from intergenic regions and introns [17,18]. Introns are recognized as a significant source of functional non coding RNAs (ncRNAs) including microRNAs (miRNAs) [18]. Moreover, a recent report implied the role of some large intronic RNAs in the pathogenesis of several types of malignancies [19]. Thus, analysis of transcripts originating from introns might be valuable for elucidating the genetic traits of HCC. We therefore focused on the transcriptional start sites potentially initiated from the intron and deregulated in HCC using 5′SAGE data. We identified that 97% of 5′SAGE tags annotated by the RefSeq database matched the sequences in the exons, while 3% matched those in the introns (1257 in the N library, 1225 in the NT library, and 1261 in the T library) (Table 4a). To identify the possible promoter regions located in the intron, we clustered the different SAGE tags to a certain genomic region if these tags positioned within 500 bp intervals (Supplemental Fig. 3), as described previously [12].

Table 1
Experimental matching of 5′SAGE tags to genome.

	Normal liver	Non-tumor	Tumor	Total
All tags	75,268	75,573	75,993	226,834
Tags mapped to genome (%)				
1 locus/genome	51,076 (71.2)	47,200 (68.0)	48,503 (68.5)	146,779 (69.3)
Multiple loci/genome	20,608 (28.8)	22,142 (32.0)	22,289 (31.5)	65,039 (30.7)
Total tags	71,684 (100)	69,342 (100)	70,792 (100)	211,818 (100)
Unique tags mapped to genome (%)				
1 locus/genome	20,736 (65.5)	20,487 (60.2)	23,753 (60.7)	64,976 (62.0)
Multiple loci/genome	10,914 (34.5)	13,548 (39.8)	15,382 (39.3)	39,844 (38.0)
Total tags	31,650 (100)	34,035 (100)	39,135 (100)	104,820 (100)
Total tags to RefSeq	45,601	39,858	41,265	126,724
Unique gene	4397	5194	6304	8410

5′SAGE indicates 5′-end serial analysis of gene expression.

Table 2
The highly expressed genes in the NL library and corresponding expression in the NT and T libraries (top 50 from NL library).

Tag count			Ratio		Gene
NL	NT	T	NT/NL	T/NL	
3731	1716	2328	0.460	0.624	Albumin (ALB)
2484	2146	2042	0.864	0.822	Apolipoprotein C-I (APOC1)
1955	1603	1079	0.820	0.552	Apolipoprotein A-II (APOA2)
1653	1050	828	0.635	0.501	Apolipoprotein A-I (APOA1)
1252	1908	1203	1.524	0.961	Transthyretin (prealbumin, amyloidosis type I) (TTR)
1233	724	220	0.587	0.178	Serpin peptidase inhibitor, clade A, member 1 (SERPINA1)
1027	872	19	0.849	0.019	Metallothionein 2A (MT2A)
755	1144	762	1.515	1.009	Ferritin, light polypeptide (FTL)
713	632	680	0.886	0.954	Alpha-1-microglobulin/bikunin precursor (AMBP)
635	524	1336	0.825	2.104	Apolipoprotein E (APOE)
631	329	57	0.521	0.090	Haptoglobin (HP)
600	228	212	0.380	0.353	Fibrinogen gamma chain (FGG)
549	395	302	0.719	0.550	Apolipoprotein C-III (APOC3)
547	644	11	1.177	0.020	Metallothionein 1X (MT1X)
479	257	290	0.537	0.605	Tumor protein, translationally-controlled 1 (TPT1)
463	217	53	0.469	0.114	Serpin peptidase inhibitor, clade A, member 3 (SERPINA3)
393	204	206	0.519	0.524	Ribosomal protein L26 (RPL26)
392	169	2	0.431	0.005	Metallothionein 1G (MT1G)
372	1011	1768	2.718	4.753	Ribosomal protein S29 (RPS29)
306	163	223	0.533	0.729	Ribosomal protein S27 (RPS27)
279	135	159	0.484	0.570	Ribosomal protein S16 (RPS16)
275	340	2	1.236	0.007	Metallothionein 1E (MT1E)
269	170	246	0.632	0.914	Ribosomal protein S23 (RPS23)
260	142	92	0.546	0.354	Fibrinogen beta chain (FGB)
260	200	195	0.769	0.750	Aldolase B, fructose-bisphosphate (ALDOB)
255	228	286	0.894	1.122	Ribosomal protein S12 (RPS12)
248	162	198	0.653	0.798	Ribosomal protein S14 (RPS14)
246	175	70	0.711	0.285	Interferon induced transmembrane protein 3 (IFITM3)
239	198	273	0.828	1.142	Ribosomal protein L31(RPL31)
229	264	0	1.153	0.004	Hepcidin antimicrobial peptide (HAMP)
228	149	156	0.654	0.684	Ribosomal protein S20 (RPS20)
222	191	117	0.860	0.527	Ubiquitin B (UBB)
216	218	352	1.009	1.630	Ribosomal protein L41 (RPL41)
210	150	155	0.714	0.738	Ribosomal protein, large, P1(RPLP1)
201	110	90	0.547	0.448	Ribosomal protein, large, P2 (RPLP2)
198	102	64	0.515	0.323	Fibrinogen alpha chain (FGA)
196	143	408	0.730	2.082	Ribosomal protein L37 (RPL37)
192	123	56	0.641	0.292	Ribosomal protein L37a (RPL37A)
191	208	346	1.089	1.812	Ribosomal protein L30 (RPL30)
174	109	76	0.626	0.437	Ribosomal protein L35 (RPL35)
169	208	3	1.231	0.018	Cytochrome P450, family 2, subfamily E, polypeptide 1 (CYP2E1)
167	105	300	0.629	1.796	Apolipoprotein H (beta-2-glycoprotein I) (APOH)
162	106	33	0.654	0.204	Serum amyloid A4, constitutive (SAA4)
159	85	157	0.535	0.987	Ribosomal protein L34 (RPL34)
159	113	229	0.711	1.440	Transferrin (TF)
155	84	135	0.542	0.871	Ribosomal protein S11 (RPS11)
152	125	101	0.822	0.664	Ribosomal protein S13 (RPS13)
147	84	1	0.571	0.007	Nicotinamide *N*-methyltransferase (NNMT)
147	180	35	1.224	0.238	Hemopexin (HPX)
146	89	121	0.610	0.829	Alpha-2-HS-glycoprotein (AHSG)

To avoid division by 0, a tag value of 1 for any tag that was not detectable was used.
NL, normal liver; NT, non-tumor; T, tumor.

More than 2 tags were detected in the intronic regions of the 164 genes in the NL, 168 genes in the NT, and 157 genes in the T library, suggesting that these regions might be potential intronic promoter regions (Table 4a). The biological process of these intron origin transcripts using Human Protein Reference Database (http://www.hprd.org/) showed that these were related to basic cellular functions such as signal transduction, transport, and regulation of the nucleobase and nucleotide, suggesting that these intronic transcripts

Table 3a
Differently expressed genes in HCC (top 10 from 5′SAGE).

5′SAGE	3′SAGE	5′/3′	Gene
T/NL	T/NL	Ratio	
Up-regulated gene			
19	6	3.17	P antigen family, member 2 (prostate associated) (PAGE2)
18	10	1.8	Lectin, galactoside-binding, soluble, 4 (LGALS4)
16	3	5.33	Choline phosphotransferase 1 (CHPT1)
14	2	7	X antien family, member 1A (XAGE1A)
14	2	7	Dehydrogenase/reductase (SDR family) member 4 (DHRS4)
14	2	7	Sterol-C5-desaturase-like (SC5DL)
13	0.5	26	Coagulation factor XIII, B polypeptide (F13B)
13	2.33	5.58	Retinol dehydrogenase 11 (all-trans and 9-cis) (RDH11)
13	0.5	26	Transmembrane protein 14A (TMEM14A)
12	1.33	9.02	Dual specificity phosphatase 23 (DUSP23)
Down-regulated gene			
0.00436	0.0137	0.318	Hepcidin antimicrobial peptide (HAMP)
0.0051	ND		Metallothionein 1G (MT1G)
0.0068	0.04	0.17	Nicotinamide *N*-methyltransferase (NNMT)
0.00727	ND		Metallothionein 1E (functional) (MT1E)
0.0098	0.0526	0.186	C-reactive protein, pentraxin-related (CRP)
0.0145	ND		Metallothionein 1 M (MT1M)
0.0152	ND		Phospholipase A2, group IIA (platelets, synovial fluid) (PLA2G2A)
0.0178	0.111	0.16	Cytochrome P450, family 2, subfamily E, polypeptide 1 (CYP2E1)
0.0185	0.192	0.096	Metallothionein 2A (MT2A)
0.0201	ND		Metallothionein 1X (MT1X)

3′SAGE, 3′-end serial analysis of gene expression; 5′SAGE, 5′-end serial analysis of gene expression; HCC, hepatocellular carcinoma; NL, normal liver; T, tumor.

may play a fundamental role in the liver (data not shown). Among these genes, 12 were differentially expressed between the NL and T libraries more than four fold (Table 4b). Interestingly, intronic transcripts (determined by 5′SAGE) of genes encoding *SAMD3*,

Table 3b
Differently expressed genes in HCC (top 10 from 3′SAGE).

5′SAGE	3′SAGE	5′/3′	Gene
T/NL	T/NL	Ratio	
Up-regulated gene			
ND	15		Leukocyte immunoglobulin-like receptor, subfamily B, member 1 (LILRB1)
ND	12		Fibroblast growth factor 5 (FGF5)
1	11	0.909	Adenosine deaminase, tRNA-specific 1 (ADAT1)
5	11	0.454	px19-like protein (PRELID1)
4.4	11	0.4	Anaphase promoting complex subunit 11 (ANAPC11)
ND	10.3		Chromosome 21 open reading frame 77 (C21orf77)
ND	10		von Willebrand factor (VWF)
2.333	10	0.233	ATX1 antioxidant protein 1 homolog (yeast) (ATOX1)
18	10	1.8	Lectin, galactoside-binding, soluble, 4 (LGALS4)
ND	9.5		Solute carrier family 26 (sulfate transporter), member 2 (SLC26A2)
Down-regulated gene			
0.5	0.012	41.7	ELL associated factor 1 (EAF1)
0.5	0.0137	36.5	TGF beta-inducible nuclear protein 1 (NSA2)
0.000436	0.0137	0.032	Hepcidin antimicrobial peptide (HAMP)
1	0.0179	55.9	Basic, immunoglobulin-like variable motif containing (BIVM)
ND	0.0182		DNA fragmentation factor, 45 kDa, alpha polypeptide (DFFA)
1	0.0185	54.1	GRIP1 associated protein 1 (GRIPAP1)
ND	0.0189		Nuclear factor of activated T-cells 5, tonicity-responsive (NFAT5)
1	0.0204	49	Adenylate cyclase 1 (ADCY1)
0.333	0.0312	10.7	Dihydroorotate dehydrogenase (DHODH)
0.738	0.0312	23.7	Ribosomal protein, large, P1 (RPLP1)

3′SAGE, 3′-end serial analysis of gene expression; 5′SAGE, 5′-end serial analysis of gene expression; HCC, hepatocellular carcinoma; NL, normal liver; T, tumor.

Table 4a
Number of 5′SAGE tags mapped to intronic region.

	NL	NT	T
Tag mapped to intron	1287	1253	1292
Total promoter region	952	981	1020
(tag number = 1)	788	813	863
(tag number ≧2)	164	168	157

ACOX2, *HGD*, *CYP3A5*, *KNG1* and *AGXT* were increased, while their 3′ transcripts (determined by 3′SAGE) were decreased in HCC. In contrast, both 5′ intronic transcripts and 3′ transcripts encoding *HFM1*, *SERPINA1*, *SUPT3H*, *A2M* and *TMEM176B* were similarly decreased in HCC. Taken together, these data imply that the canonical and intronic promoter activities of a subset of genes including *SAMD3*, *ACOX2*, *HGD*, *CYP3A5*, *KNG1* and *AGXT* might be differently regulated in HCC.

ACOX2 as a novel intronic gene deregulated in HCC

A subset of genes listed above may be transcribed from intronic regions specifically in HCC. Among these genes, we focused on the regulation of *ACOX2*, which is reported to be potentially involved in peroxisomal beta oxidation and hepatocarcinogenesis [20]. The intron origin expression of *ACOX2* increased six fold in HCC compared with the NT by 5′SAGE, while the expression based on the 3′end was almost similar between HCC and NT lesions (Table 4b). Close examination of 5′SAGE data identified two potential intron origin transcripts of *ACOX2* (Supplemental Fig. 4). The first (intronic *ACOX2 1*) was initiated upstream of the tenth exon, whereas the second (intronic *ACOX2 2*) was initiated upstream of the twelfth exon of *ACOX2* (Supplemental Fig. 4). The sequence of the intronic part was unique, and the remaining part of the sequence was shared with the canonical transcripts of *ACOX2*.

The expression of canonical *ACOX2* and the two types of intron origin transcripts was investigated in NL, NT, and T tissues by RT PCR (Fig. 1A). Although canonical *ACOX2* expression was decreased in T than in NL, the intron origin transcript, particularly intronic *ACOX2 1*, was increased in T. Intronic *ACOX2 2* transcripts also showed a modest increase. We further evaluated the alteration of these transcripts in 19 HBV HCCs, 20 HCV HCCs, and 4 non B, non C HCCs, and their background liver tissues by canonical *ACOX2* and intronic *ACOX2* specific real time detection (RTD) PCR. Although the expression of canonical *ACOX2* was decreased, the expression of intronic *ACOX2* was significantly increased (Fig. 1B). Importantly, the gene expression ratios of intronic to canonical *ACOX2* increased more in moderately differentiated HCCs (mHCC) than in well differentiated HCCs (wHCC), suggesting the involvement of intronic *ACOX2* expres sion on HCC progression.

Table 4b
Differentially expressed intronic promoter regions in HCC.

5′SAGE T/NL	3′SAGE T/NL	5′/3′ Ratio	Gene
Up-regulated			
9	1	9.00	Sterile alpha motif domain containing 3 (SAMD3)
6	0.89	6.74	Acyl-Coenzyme A oxidase 2, branched chain (ACOX2)
6	0.62	9.68	Homogentisate 1,2-dioxygenase (homogentisate oxidase) (HGD)
6	0.009	666.67	Cytochrome P450, family 3, subfamily A, polypeptide 5 (CYP3A5)
5	0.64	7.81	Kininogen 1 (KNG1)
4	0.36	11.11	Alanine-glyoxylate aminotransferase (AGXT)
4	1	4.00	Crystallin, alpha A (CRYAA)
Down-regulated			
0.13	1	0.13	HFM1, ATP-dependent DNA helicase homolog (*S. cerevisiae*) (HFM1)
0.25	0.51	0.49	Serpin peptidase inhibitor, clade A member 1 (SERPINA1)
0.25	1	0.25	Suppressor of Ty 3 Homolog (*S. cerevisiae*) (SUPT3H)
0.25	0.2	1.25	Alpha-2-macroglobulin (A2M)
0.25	0.083	3.13	Transmembrane protein 176B (TMEM176B)

3′SAGE, 3′-end serial analysis of gene expression; 5′SAGE, 5′-end serial analysis of gene expression; HCC, hepatocellular carcinoma; NL, normal liver; NT, non-tumor; T, tumor.

Discussion

This is the first comprehensive transcriptional analysis of tissue lesions of non B, non C HCC, background liver and NL using the 5′ SAGE method. Approximately 6.7% of our 5′SAGE tags showed no matching within the human genome, possibly due to the presence of a single nucleotide polymorphism (SNP) in the human genome. Out of the complete matched tags in the genome, 70% were assigned to unique positions and 30% to two or more loci. The tags with multiple matches with genomic loci were largely retrotransposon elements, repetitive sequences, and pseudogenes.

In this study, the analysis of non B, non C HCC enabled us to evaluate direct molecular changes associated with HCC without any bias of gene induction by virus infection. The gene expression profile based on our 5′SAGE tags revealed that *albumin (ALB)* and apolipoproteins were highly expressed in NL, indicating the massive production of plasma proteins in NL; these results are similar to those of our previous study using 3′SAGE [6]. Other genes such as *aldolase B (ALDOB)*, *antitrypsin (SERPINA1)*, and *haptoglobin (HP)* were also highly expressed in NL, in both the 5′SAGE and 3′SAGE libraries (Table 2) [6]. Comparison of the expression profiles among NL, background NT and T identified several differentially expressed transcripts in T. *Galectin 4 (LGALS4)* was up regulated and *HAMP*, *NNMT*, *CYP2E1*, and *metallothionein* were down regulated in HCC in accordance with previous findings (Table 3a) [8,9,21]. Moreover, *CLEC4G*, which was predominantly expressed in the sinusoidal endothelial cells of the liver, was down regulated in HCC. In addition, we first found that *P antigen family, member 2 (PAGE2)* and *XAGE1A* were up regulated in HCC (Table 3a, Supplemental Fig. 1). These genes were members of cancer testis antigen that include MAGE family genes. MAGE family members were originally found to be up regulated in HCV related HCC, and reported to be useful as molecular markers and as possible target molecules for immunotherapy in human HCC [22]. In this study, we identified that these members of genes were also up regulated in non B, non C HCC. Thus, these genes may be useful as molecular markers and therapeutic targets for the treatment of a certain type of human HCC.

There existed some discrepancy between 5′SAGE and 3′SAGE results, even though they were derived from the same sample. Technical issues such as amplication error, difference of restriction enzyme, and annotation error have been described previously [14]. It is possible that 3′ transcripts might be more stable than 5′ transcripts by binding of ribosomal proteins during translation. Another possibility is the diversity of the transcriptional start and/or termination sites. One of the advantages of 5′SAGE analysis is the potential to determine the transcriptional start sites in each gene. Indeed, a recent study indicated the importance of an insulin splice variant in the pathogenesis of insulinomas [23]. Considering the diversity of 5′ends of genes, it is more appropriate to perform 5′SAGE in combination with 3′SAGE when determining the frequency of gene expression and identifying novel transcript variants.

Here, we were able to identify at least 12 intron origin transcripts that were differentially expressed in HCC compared with the background liver or NL. These transcripts could not be identified by the 3′SAGE approach. We also performed detailed expression analysis of *ACOX2* that was involved in the beta oxidation of peroxisome. We

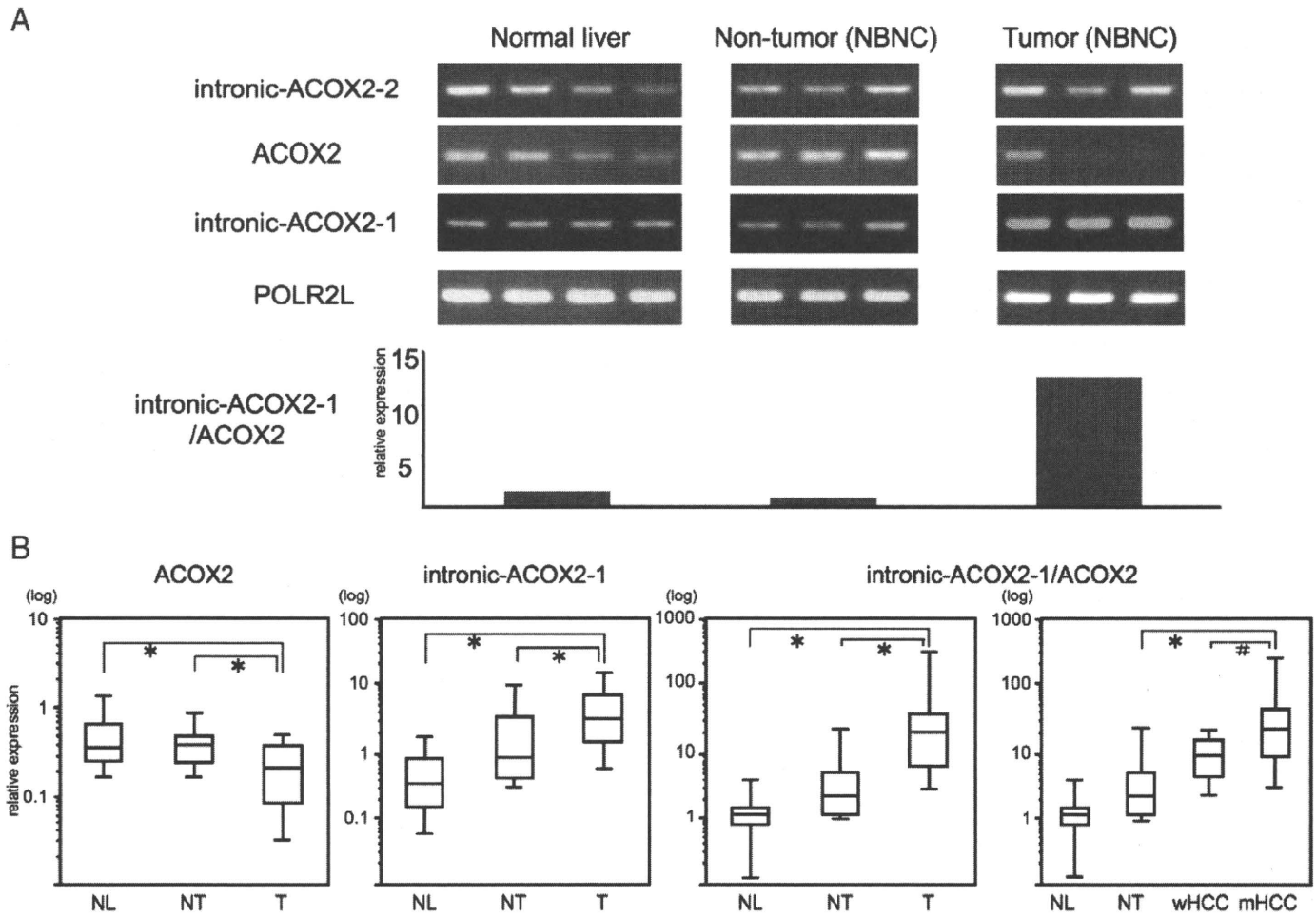

Fig. 1. (A) RT-PCR results of *ACOX2* and *ACOX2* intronic RNAs in independent NL, NT (non-B, non-C), and T (non-B, non-C) samples. RT-PCR was performed in triplicate for each sample-primer set from cDNA. The PCR products were semi-quantitatively analyzed with ImageJ software and calculated as levels relative to *polymerase (RNA) II (DNA directed) polypeptide L (POLR2L)*. The bar graph indicates the expression ratio of intronic-ACOX2-1 to canonical ACOX2. The expression pattern of intron 1 was different from that of canonical *ACOX2*. (B) RTD-PCR analysis of *ACOX2* and *ACOX2* intronic RNAs in NL, T (HBV-related, HCV-related, and non-B, non-C), and NT tissues. Quantitative RTD-PCR was performed in duplicate for each sample-primer set from cDNA. Each sample was normalized relative to *POLR2L*. All HCC tissues were pathologically diagnosed as well differentiated HCC (wHCC) or moderately differentiated HCC (mHCC). Kruskal–Wallis tests and Mann–Whitney *U* tests were used for statistical analysis. ACOX2, acyl-Coenzyme A oxidase 2; HCC, hepatocellular carcinoma; NL, normal liver; NT, non-tumor; RT-PCR, reverse transcriptase-polymerase chain reaction; RTD-PCR, real-time detection-PCR; T, tumor. $^{*}P<0.01$, $\#P<0.05$.

were able to clone the intron origin *ACOX2* RNAs (intronic *ACOX2 1, 2*) for the first time and found that intronic *ACOX2 1* was significantly overexpressed in T compared with NT and NL. The ratio of intronic *ACOX2 1* and canonical *ACOX2* (relative intronic *ACOX2*) was progres sively up regulated from NL via the background liver to HCC. Importantly, the expression of relative intronic *ACOX2* was more up regulated in moderately differentiated HCC than in well differentiated HCC. The intronic difference in expression might be due to a poly morphism, since the 5′SAGE library for NL and T were from different people. The mechanisms of stepwise increase of intronic *ACOX2* in the process of hepatocarinogenesis should be clarified in future.

ACOX2 is a rate limiting enzyme of branched chain acyl CoA oxidase involved in the degradation of long branched fatty acid and bile acid intermediates in peroxisomes. *ACOX2* expression was associated with the differentiation state of hepatocytes and was repressed under the undifferentiated phase of human hepatoma cell lines [24]. A decreased *ACOX2* expression was also reported in prostate cancer [25]. Here, the expression of canonical *ACOX2* was decreased, while that of intronic *ACOX2 1* was increased in HCC. The deduced amino acid of intronic *ACOX2 1* encodes the C terminal (from 386 to 681 amino acids) of canonical *ACOX2*, lacking the active sites for FAD binding and a fatty acid as the substrate, suggesting that the protein may be functionally departed [26]. The biological role of the increased intronic *ACOX2 1* was not clear, but it might be reflected by the activation of peroxisome proliferators activated receptor alpha (PPARA). It is reported that mice lacking ACOX1, another rate limiting enzyme in peroxisomal straight chain fatty acid oxidation, developed steatosis and HCC characterized by increased mRNA and protein expression of genes regulated by PPARα [27]. The importance of PPARα activation in HCC development has been recently reported using HCV core protein transgenic mice [28]. Moreover, the overexpression of alpha methylacyl CoA racemase (AMACR), an enzyme for branched chain fatty acid beta oxidation, is reported to be a reliable diagnostic marker of prostate cancer and is associated with the decreased expression of ACOX2 [25]. Therefore, the expression of intronic *ACOX2 1* might open the door for further investigations of their potential clinical use, e.g., serving as diagnostic markers of HCC, although the functional relevance of this gene should be further clarified.

In conclusion, we report the first comprehensive transcriptional analysis of non B, non C HCC, NT background liver, and NL tissue, based on 5′SAGE. This study offers new insights into the transcrip tional changes that occur during HCC development as well as the molecular mechanism of carcinogenesis in the liver. The results suggest the presence of unique intron origin RNAs that are useful as diagnostic markers and may be used as new therapeutic targets.

Material and methods

Samples

Samples were obtained from a 56 year old man who had undergone surgical hepatic resection for the treatment of solitary HCC. Serological tests for hepatitis B surface (HBs) antigen and anti HCV antibodies were negative. Tumor (T) and non tumor (NT) tissue samples were separately obtained from the tumorous parts (diagnosed as moderately differentiated HCC) and non tumorous parts (diagnosed as mild chronic hepatitis: F1A1) of the resected tissue. We also obtained five normal liver (NL) tissue samples from five patients who had undergone surgical hepatic resection because of metastatic liver cancer. None of the patients was seropositive for both HBs antigen and anti HCV antibodies. Neither heavy alcohol consumption nor the intake of chemical agents was observed before surgical resection. All laboratory values related to hepatic function were within the normal range. All procedures and risks were explained verbally and provided in a written consent form.

We additionally used independent four NL tissue samples, 19 HBV HCCs, 20 HCV HCCs and 4 non B, non C HCCs, and their background liver tissue samples for reverse transcriptase polymerase chain reaction (RT PCR) and real time detection (RTD) PCR (Supplemental Table 1). Four non B, non C HCCs were histologically diagnosed as moderately differentiated HCCs, and the adjacent non cancerous liver tissues were diagnosed as a normal liver, a chronic hepatitis, a pre cirrhotic liver and a cryptogenic liver cirrhosis, respectively. None of the patients was seropositive for HBs antigen, anti HBs antibodies, anti hepatitis B core (HBc) antibodies and anti HCV antibodies. Neither heavy alcohol consumption nor the intake of chemical agents was observed. Histological grading of the tumor was evaluated by two independent pathologists as described previously [16].

Generation of the 5′ SAGE library

5′SAGE libraries were generated as previously described [14]. Five to ten micrograms of poly(A)+RNA was treated with bacterial alkaline phosphatase (BAP; TaKaRa, Otsu, Japan). Poly(A)+RNA was extracted twice with phenol: chloroform (1:1), ethanol precipitated, and then treated with tobacco acid pyrophosphatase (TAP). Two to four micrograms of the BAP TAP treated poly(A)+RNA was divided into two aliquots and an RNA linker containing recognition sites for *Eco*RI/*Mme*I was ligated using RNA ligase (TaKaRa): one aliquot was ligated to a 5′ oligo 1 (5′ GGA UUU GCU GGU GCA GUA CAA CGA AUU CCG AC 3′) linker, and the other aliquot was ligated to a 5′ oligo 2 (5′ CUG CUC GAA UGC AAG CUU CUG AAU UCC GAC 3′) linker. After removing unligated 5′ oligo, cDNA was synthesized using RNaseH free reverse transcriptase (Superscript II, Invitrogen, Carlsbad, CA, USA) at 12 °C for 1 h and 42 °C for the next hour, using 10 pmol of dT adapter primer (5′ GCG GCT GAA GAC GGC CTA TGT GGC CTT TTT TTT TTT TTT TTT 3′). After first strand synthesis, RNA was degraded in 15 mM NaOH at 65 °C for 1 h. cDNA was amplified in a volume of 100 μl by PCR with 16 pmol of 5′ (5′ [biotin] GGA TTT GCT GGT GCA GTA CAA 3′ or 5′[biotin] CTG CTC GAA TGC AAG CTT CTG 3′) and 3′ (5′ GCG GCT GAA GAC GGC CTA TGT 3′) PCR primers. cDNA was amplified using 10 cycles at 94 °C for 1 min, 58 °C for 1 min, and 72 °C for 2 min. PCR products were digested with the *Mme*I type IIS restriction endonuclease (NEB, Pickering, Ontario, Canada). The digested 5′ terminal cDNA fragments were bound to streptavidin coated magnetic beads (Dynal, Oslo, Norway). cDNA fragments that bound to the beads were directly ligated together in a reaction mixture containing T4 DNA ligase in a supplied buffer for 2.5 h at 16 °C. The ditags were amplified by PCR using the following primers: 5′ GGA TTT GCT GGT GCA GTA CA 3′ and 5′ CTG CTC GAA TGC AAG CTT CT 3′. The PCR products were analyzed by polyacrylamide gel electrophoresis (PAGE) and digested with *Eco*RI. The region of the gel containing the ditags was excised and the fragments were self ligated to produce long concatamers that were then cloned into the *Eco*RI site of pZero 1.0 (Invitrogen). Colonies were screened by PCR using the M13 forward and reverse primers. PCR products containing inserts of more than 600 bp were sequenced with Big Dye terminator ver.3 and analyzed using a 3730 ABI automated DNA sequencer (Applied Biosystems, Foster City, CA, USA). All electrophoretograms were reanalyzed by visual inspection to check for ambiguous bases and to correct misreads. In this study, we obtained 19 20 bp tag information.

Association of the 5′SAGE tags with their corresponding genes

We attempted to align our 5′tags with the human genome (NCBI build 36, available from http://www.genome.ucsc.edu/) using the alignment program ALPS (http://www.alps.gi.k.u tokyo.ac.jp/). Only tags that matched in sense orientation were considered in our analysis. The RefSeq database was searched for transcripts corresponding to the regions adjacent to the alignment location of each 5′tag.

RT PCR

Total RNA was extracted using a ToTally RNA extraction kit (Ambion, Inc., Austin, TX, USA). Total RNA (500 ng) was reverse transcribed in a 100 μl reaction solution containing 240 U of Moloney murine leukemia virus reverse transcriptase (Promega, Madison, WI, USA), 80 U of RNase inhibitor (Promega), 4.6 mM $MgCl_2$, 6.6 mM DTT, 1 mM dNTPs, and 2 mM random hexamer (Promega), at 42 °C for 1 h. PCR was performed in a 20 μl volume containing 0.5 U of AmpliTaq DNA polymerase (Applied Biosystems), 16.6 mM $(NH_4)_2SO_4$, 67 mM Tris HCl, 6.7 mM $MgCl_2$, 10 mM 2 mercaptoethanol, 1 mM dNTPs, and 1.5 μM sense and antisense primers, using an ABI 9600 thermal cycler (Applied Biosystems). The amplification protocol included 28 30 cycles of 95 °C for 45 s, 58 °C for 1 min, and 72 °C for 1 min. Primer sequences are shown in Supplemental Table 2. RT PCR was performed in triplicate for each sample primer set. Each sample was normalized relative to *polymerase (RNA) II (DNA directed) polypeptide L (POLR2L)*. *POLR2L* is a housekeeping gene that showed relatively stable gene expression in various tissues [29]. The PCR products were semi quantitatively analyzed with ImageJ software (http://rsb.info.nih.gov/ij/).

RTD PCR

Intron origin transcript expression was quantified using TaqMan Universal Master Mix (Applied Biosystems). The samples were amplified using an ABI PRISM 7900HT Sequence Detection System (Applied Biosystems). Using the standard curve methods, quantitative PCR was performed in duplicate for each sample primer set. Each sample was normalized relative to *POLR2L*. The assay IDs used were Hs00185873_m1 for *ACOX2* and Hs00360764_m1 for *POLR2L*. The specific primers and probe sequence of intronic *ACOX2 1* were 5′ TTCATAAAGTTGTGAGCA GAGGAAA 3′ (forward), 5′ TGCACCACTTACTGAGCATCTACTC 3′ (reverse), and 5′ ACTTCTTACCTCAGAGCTG 3′ (probe).

Analysis of pathway network

MetaCore™ software (GeneGo Inc., St. Joseph, MI) was used to investigate the molecular pathway networks of non B, non C HCC, HBV HCC and HCV HCC. All genes up regulated more than five fold in all HCC libraries subjected to Enrichment analysis in GO process networks by default settings ($p<0.05$).

Statistical analysis

Kruskal Wallis tests were used to compare the expression among normal liver, non cancerous tissues, and HCC tissues. Mann Whitney *U* tests were also used to evaluate the statistical significance of ACOX2

gene expression levels between two groups. All statistical analyses were performed using R (http://www.r project.org/).

Acknowledgments

The authors would like to thank Mr. Shungo Deshimaru and Ms. Keiko Harukawa for technical assistance.

Appendix A. Supplementary data

Supplementary data associated with this article can be found, in the online version, at doi:10.1016/j.ygeno.2010.01.004.

References

[1] H.B. El-Serag, K.L. Rudolph, Hepatocellular carcinoma: epidemiology and molecular carcinogenesis, Gastroenterology 132 (2007) 2557–2576.
[2] Y. Yokoi, S. Suzuki, S. Baba, K. Inaba, H. Konno, S. Nakamura, Clinicopathological features of hepatocellular carcinomas (HCCs) arising in patients without chronic viral infection or alcohol abuse: a retrospective study of patients undergoing hepatic resection, J. Gastroenterol. 40 (2005) 274–282.
[3] R.N. Aravalli, C.J. Steer, E.N. Cressman, Molecular mechanisms of hepatocellular carcinoma, Hepatology 48 (2008) 2047–2063.
[4] D.J. Duggan, M. Bittner, Y. Chen, P. Meltzer, J.M. Trent, Expression profiling using cDNA microarrays, Nat. Genet. 21 (1999) 10–14.
[5] V.E. Velculescu, L. Zhang, B. Vogelstein, K.W. Kinzler, Serial analysis of gene expression, Science 270 (1995) 484–487.
[6] T. Yamashita, S. Hashimoto, S. Kaneko, S. Nagai, N. Toyoda, T. Suzuki, K. Kobayashi, K. Matsushima, Comprehensive gene expression profile of a normal human liver, Biochem. Biophys. Res. Commun. 269 (2000) 110–116.
[7] S. Hashimoto, S. Nagai, J. Sese, T. Suzuki, A. Obata, T. Sato, N. Toyoda, H.Y. Dong, M. Kurachi, T. Nagahata, K. Shizuno, S. Morishita, K. Matsushima, Gene expression profile in human leukocytes, Blood 101 (2003) 3509–3513.
[8] H. Okabe, S. Satoh, T. Kato, O. Kitahara, R. Yanagawa, Y. Yamaoka, T. Tsunoda, Y. Furukawa, Y. Nakamura, Genome-wide analysis of gene expression in human hepatocellular carcinomas using cDNA microarray: identification of genes involved in viral carcinogenesis and tumor progression, Cancer. Res. 61 (2001) 2129–2137.
[9] Y. Shirota, S. Kaneko, M. Honda, H.F. Kawai, K. Kobayashi, Identification of differentially expressed genes in hepatocellular carcinoma with cDNA microarrays, Hepatology 33 (2001) 832–840.
[10] T. Yamashita, M. Honda, S. Kaneko, Application of serial analysis of gene expression in cancer research, Curr. Pharm. Biotechnol. 9 (2008) 375–382.
[11] Y. Suzuki, H. Taira, T. Tsunoda, J. Mizushima-Sugano, J. Sese, H. Hata, T. Ota, T. Isogai, T. Tanaka, S. Morishita, K. Okubo, Y. Sakaki, Y. Nakamura, A. Suyama, S. Sugano, Diverse transcriptional initiation revealed by fine, large-scale mapping of mRNA start sites, EMBO Rep. 2 (2001) 388–393.
[12] K. Kimura, A. Wakamatsu, Y. Suzuki, T. Ota, T. Nishikawa, R. Yamashita, J. Yamamoto, M. Sekine, K. Tsuritani, H. Wakaguri, S. Ishii, T. Sugiyama, K. Saito, Y. Isono, R. Irie, N. Kushida, T. Yoneyama, R. Otsuka, K. Kanda, T. Yokoi, H. Kondo, M. Wagatsuma, K. Murakawa, S. Ishida, T. Ishibashi, A. Takahashi-Fujii, T. Tanase, K. Nagai, H. Kikuchi, K. Nakai, T. Isogai, S. Sugano, Diversification of transcriptional modulation: large-scale identification and characterization of putative alternative promoters of human genes, Genome. Res. 16 (2006) 55–65.
[13] T. Shiraki, S. Kondo, S. Katayama, K. Waki, T. Kasukawa, H. Kawaji, R. Kodzius, A. Watahiki, M. Nakamura, T. Arakawa, S. Fukuda, D. Sasaki, A. Podhajska, M. Harbers, J. Kawai, P. Carninci, Y. Hayashizaki, Cap analysis gene expression for high-throughput analysis of transcriptional starting point and identification of promoter usage, Proc. Natl. Acad. Sci. U. S. A. 100 (2003) 15776–15781.
[14] S. Hashimoto, Y. Suzuki, Y. Kasai, K. Morohoshi, T. Yamada, J. Sese, S. Morishita, S. Sugano, K. Matsushima, 5′-end SAGE for the analysis of transcriptional start sites, Nat. Biotechnol. 22 (2004) 1146–1149.
[15] T. Yamashita, S. Kaneko, S. Hashimoto, T. Sato, S. Nagai, N. Toyoda, T. Suzuki, K. Kobayashi, K. Matsushima, Serial analysis of gene expression in chronic hepatitis C and hepatocellular carcinoma, Biochem. Biophys. Res. Commun. 282 (2001) 647–654.
[16] T. Yamashita, M. Honda, H. Takatori, R. Nishino, H. Minato, H. Takamura, T. Ohta, S. Kaneko, Activation of lipogenic pathway correlates with cell proliferation and poor prognosis in hepatocellular carcinoma, J. Hepatol. 50 (2009) 100–110.
[17] J.S. Mattick, Introns: evolution and function, Curr. Opin. Genet. Dev. 4 (1994) 823–831.
[18] J.S. Mattick, I.V. Makunin, Non-coding RNA, Hum. Mol. Genet. 15 (Spec No 1) (2006) R17–29.
[19] R. Louro, A.S. Smirnova, S. Verjovski-Almeida, Long intronic noncoding RNA transcription: expression noise or expression choice? Genomics 93 (2009) 291–298.
[20] S. Yu, S. Rao, J.K. Reddy, Peroxisome proliferator-activated receptors, fatty acid oxidation, steatohepatitis and hepatocarcinogenesis, Curr. Mol. Med. 3 (2003) 561–572.
[21] N. Kondoh, T. Wakatsuki, A. Ryo, A. Hada, T. Aihara, S. Horiuchi, N. Goseki, O. Matsubara, K. Takenaka, M. Shichita, K. Tanaka, M. Shuda, M. Yamamoto, Identification and characterization of genes associated with human hepatocellular carcinogenesis, Cancer. Res. 59 (1999) 4990–4996.
[22] Y. Kobayashi, T. Higashi, K. Nouso, H. Nakatsukasa, M. Ishizaki, T. Kaneyoshi, N. Toshikuni, K. Kariyama, E. Nakayama, T. Tsuji, Expression of MAGE, GAGE and BAGE genes in human liver diseases: utility as molecular markers for hepatocellular carcinoma, J. Hepatol. 32 (2000) 612–617.
[23] A.H. Minn, M. Kayton, D. Lorang, S.C. Hoffmann, D.M. Harlan, S.K. Libutti, A. Shalev, Insulinomas and expression of an insulin splice variant, Lancet 363 (2004) 363–367.
[24] H. Stier, H.D. Fahimi, P.P. Van Veldhoven, G.P. Mannaerts, A. Volkl, E. Baumgart, Maturation of peroxisomes in differentiating human hepatoblastoma cells (HepG2): possible involvement of the peroxisome proliferator-activated receptor alpha (PPAR alpha), Differentiation 64 (1998) 55–66.
[25] S. Zha, S. Ferdinandusse, J.L. Hicks, S. Denis, T.A. Dunn, R.J. Wanders, J. Luo, A.M. De Marzo, W.B. Isaacs, Peroxisomal branched chain fatty acid beta-oxidation pathway is upregulated in prostate cancer, Prostate 63 (2005) 316–323.
[26] K. Tokuoka, Y. Nakajima, K. Hirotsu, I. Miyahara, Y. Nishina, K. Shiga, H. Tamaoki, C. Setoyama, H. Tojo, R. Miura, Three-dimensional structure of rat-liver acyl-CoA oxidase in complex with a fatty acid: insights into substrate-recognition and reactivity toward molecular oxygen, J. Biochem. 139 (2006) 789–795.
[27] K. Meyer, Y. Jia, W.Q. Cao, P. Kashireddy, M.S. Rao, Expression of peroxisome proliferator-activated receptor alpha, and PPARalpha regulated genes in spontaneously developed hepatocellular carcinomas in fatty acyl-CoA oxidase null mice, Int. J. Oncol. 21 (2002) 1175–1180.
[28] N. Tanaka, K. Moriya, K. Kiyosawa, K. Koike, F.J. Gonzalez, T. Aoyama, PPARalpha activation is essential for HCV core protein-induced hepatic steatosis and hepatocellular carcinoma in mice, J. Clin. Invest. 118 (2008) 683–694.
[29] C. Rubie, K. Kempf, J. Hans, T. Su, B. Tilton, T. Georg, B. Brittner, B. Ludwig, M. Schilling, Housekeeping gene variability in normal and cancerous colorectal, pancreatic, esophageal, gastric and hepatic tissues, Mol. Cell. Probes. 19 (2005) 101–109.